

33044



National Library of Canada

Bibliothèque nationale du Canada

CANADIAN THESES ON MICROFICHE

THÈSES CANADIENNES SUR MICROFICHE

NAME OF AUTHOR/NOM DE L'AUTEUR Mr. S. B. Rao

TITLE OF THESIS/TITRE DE LA THÈSE "Analysis of the Dynamic Cutting Force Coefficient"

UNIVERSITY/UNIVERSITÉ McMaster University

DEGREE FOR WHICH THESIS WAS PRESENTED/
GRADE POUR LEQUEL CETTE THÈSE FUT PRÉSENTÉE Master of Engineering

YEAR THIS DEGREE CONFERRED/ANNÉE D'OBTENTION DE CE DEGRÉ 1977

NAME OF SUPERVISOR/NOM DU DIRECTEUR DE THÈSE Dr. J. Tlusty

Permission is hereby granted to the NATIONAL LIBRARY OF CANADA to microfilm this thesis and to lend or sell copies of the film.

L'autorisation est, par la présente, accordée à la BIBLIOTHÈQUE NATIONALE DU CANADA de microfilmer cette thèse et de prêter ou de vendre des exemplaires du film.

The author reserves other publication rights, and neither the thesis nor extensive extracts from it may be printed or otherwise reproduced without the author's written permission.

L'auteur se réserve les autres droits de publication; ni la thèse ni de longs extraits de celle-ci ne doivent être imprimés ou autrement reproduits sans l'autorisation écrite de l'auteur.

DATED/DATÉ 27th May '77 SIGNED/SIGNÉ Bhuvendra Rao

PERMANENT ADDRESS/RÉSIDENCE FIXE 276, MAHALAKSHMI LAYOUT
BANGALORE . INDIA 560 010



National Library of Canada

Cataloguing Branch
Canadian Theses Division

Ottawa, Canada
K1A 0N4

Bibliothèque nationale du Canada

Direction du catalogage
Division des thèses canadiennes

NOTICE

The quality of this microfiche is heavily dependent upon the quality of the original thesis submitted for microfilming. Every effort has been made to ensure the highest quality of reproduction possible.

If pages are missing, contact the university which granted the degree.

Some pages may have indistinct print especially if the original pages were typed with a poor typewriter ribbon or if the university sent us a poor photocopy.

Previously copyrighted materials (journal articles, published tests, etc.) are not filmed.

Reproduction in full or in part of this film is governed by the Canadian Copyright Act, R.S.C. 1970, c. C-30. Please read the authorization forms which accompany this thesis.

**THIS DISSERTATION
HAS BEEN MICROFILMED
EXACTLY AS RECEIVED**

AVIS

La qualité de cette microfiche dépend grandement de la qualité de la thèse soumise au microfilmage. Nous avons tout fait pour assurer une qualité supérieure de reproduction.

Si il manque des pages, veuillez communiquer avec l'université qui a conféré le grade.

La qualité d'impression de certaines pages peut laisser à désirer, surtout si les pages originales ont été dactylographiées à l'aide d'un ruban usé ou si l'université nous a fait parvenir une photocopie de mauvaise qualité.

Les documents qui font déjà l'objet d'un droit d'auteur (articles de revue, examens publiés, etc.) ne sont pas microfilmés.

La reproduction, même partielle, de ce microfilm est soumise à la Loi canadienne sur le droit d'auteur, SRC 1970, c. C-30. Veuillez prendre connaissance des formules d'autorisation qui accompagnent cette thèse.

**LA THÈSE A ÉTÉ
MICROFILMÉE TELLE QUE
NOUS L'AVONS REÇUE**

ANALYSIS OF THE DYNAMIC CUTTING FORCE COEFFICIENT

ANALYSIS OF THE DYNAMIC CUTTING FORCE COEFFICIENT

by

SURENDRA B. RAO

A Thesis

Submitted to the School of Graduate Studies

in Partial Fulfilment of the Requirements

for the Degree

Master of Engineering

May, 1977

Master of Engineering (1977)

McMaster University
Hamilton, Ontario

Title: Analysis of the Dynamic Cutting Force Coefficient

Author: Surendra B. Rao B.E. (Bangalore University)

Supervisor: Professor J. Tlustý

Number of Pages:

Preliminaries	ix
Text	48
Appendix	4
Figures	26 (30 figures)

TO MY PARENTS

ABSTRACT

Conclusive evidence is presented in this thesis that the Dynamic Cutting Force Coefficients, as measured by the Double Modulation Method, do indeed represent the transfer function of the cutting process. Limits of stability, computed from the measured DCFCs for various steels and the measured transfer function of a lathe, are arrived at and compared with the experimental b_{lim} obtained, with these same steels, under similar cutting conditions on the same lathe.

A physical model to explain the DCFCs of Inner Modulation is presented. Mathematical relations are derived to correlate stable cutting forces with DCFCs of Inner Modulation. Tests results of stable cutting forces are presented from which the DCFCs of Inner Modulation are obtained using the above mentioned mathematical relations. A comparison of the computed and experimentally obtained DCFCs of Inner Modulation is presented to show the validity of the proposed model.

ACKNOWLEDGEMENTS

The author wishes to express his gratitude to Professor J. Tlusty for his continuous guidance throughout the course of this work.

The financial assistance in the form of a teaching assistantship in the Department of Mechanical Engineering is gratefully acknowledged.

Thanks are also due to Miss L. Onešchuk for her expert typing of the final draft.

CONTENTS

		Page.
PRELIMINARIES	Abstract	iv
	Acknowledgements	v
	Table of Contents	vi
	Nomenclature	viii
CHAPTER 1	Introduction	1
CHAPTER 2	Literature Survey	5
2.1.1	Quasi-Experimental Methods	5
2.2	Experimental Methods	10
2.2.1	Stiffness Methods	10
2.2.2	Dynamometer Methods	12
2.3	Other Investigations on the Dynamic Cutting Process	14
CHAPTER 3	Theoretical Background, Experi- mental Equipment and Technique	19
3.1	Theoretical Background, of the Measurement of Dynamic Cutting Force Coefficients	19
3.2	Experimental Equipment	22
3.2.1	Dynamic Cutting	22
3.2.2	Stable Cutting	25
3.3	Experimental Techniques	26
3.3.1	Dynamic Cutting	26
3.3.2	Stable Cutting	28

CHAPTER 4	Results and Discussions	29
4.1	Verification of the Validity of the Measured DCFCs	29
4.2	Correlation of the DCFCs With Stable Cutting Forces	34
CHAPTER 5	Conclusions	45
REFERENCES		47
APPENDIX	Listing of Computer Program to Calculate the Stability Limit	A1
FIGURES		

NOMENCLATURE

A_P	Complex cutting force coefficient of inner modulation for thrust force
B_P	Complex cutting force coefficient of outer modulation for thrust force
A_V	Complex cutting force coefficient of inner modulation for main cutting force
B_V	Complex cutting force coefficient of outer modulation for main cutting force
b	Width of cut
b_{lim}	Limiting width of cut
C_C	Damping coefficient of cutting process
C_T	Damping coefficient of total machining system
f	Frequency
f_P	Static thrust force
f_V	Static main cutting force
F	Cutting force
F_P	Dynamic thrust force
F_V	Dynamic main cutting force
F_i	Resultant cutting force due to inner modulation
F_o	Resultant cutting force due to outer modulation
$G(\omega)$	Real part of receptance
G_{min}	Minimum value of $G(\omega)$
$I_m(K)$	Represent imaginary part of complex quantity

j	$\sqrt{-1}$
K_c	Stiffness of cutting process
l	Shear plane length
$R_e(K)$	Represent real part of complex quantity K
s	Feed rate
V	Cutting speed
V_B	Flank wear land width
X	Displacement
X_i	Amplitude of inner modulation
X_o	Amplitude of outer modulation
ϕ	Shear plane angle
ϵ	Phase angle between inner and outer modulation
ω	Frequency

CHAPTER 1
INTRODUCTION

Chatter, in machining, is a phenomenon which has attracted the attention of many research workers for several years. It is essentially, a case of Self-Excited Vibrations when the energy generated in the cutting process excites the machine tool structure to undergo vibratory motion; the motion itself leading to further vibratory energy being generated in the cutting process.

In the past, if chatter occurred when machining, the operator simply changed the cutting conditions to overcome the problem. However with the advent of automation, flexible or otherwise, where very little or no human attention is available to supervise the operation, and with the growing necessity of machines having to operate at most optimum conditions, the problem of chatter has attained great significance. More specifically, it is the need to develop the ability to correctly predict the cutting conditions under which chatter can occur, knowing the dynamic characteristics of the machine tool and the material to be operated upon. The machine tool could be then set or programmed to operate under the requisite optimum conditions, yet avoiding those conditions which could lead to unstable machining.

Thusty (1) identified the basic diagram of the process of Self-Excited Vibration as shown in Figure 1. It is a closed loop system having two fundamental parts, the cutting process and the vibratory system of the machine tool and also the mutual directional orientation of the two parts. It indicates that the vibration X between tool and workpiece influences the cutting process so as to cause a variation P of the cutting force which acting on the vibratory system of the machine, creates again vibration X .

In the past successful techniques have been established to measure the transfer function of the machine tool system. However it is only recently, owing to its complexity, that attempts have been made to obtain the transfer function of the cutting process. So in order that the above mentioned requirement, of being able to accurately predict the conditions under which chatter can occur, be met the following is necessary. "A reliable and accurate method to easily measure the transfer function of the cutting process under all cutting conditions."

It is with this end in view, that the objective of this present work was defined. They can be broadly classified as follows:

1. Using the Double-Modulation Method developed by Goel and Thusty (2,3,4), the Dynamic Cutting Force Coefficients, which represent the transfer function of the cutting

process, are measured for various steels and various cutting conditions. The validity of these coefficients is then tested by theoretically computing the limit of stability or b_{lim}^r for a machine tool whose transfer function is known, from the measured Dynamic Cutting Force Coefficients or DCFCs as they are known. The actual b_{lim} on that machine tool is experimentally determined and compared with the computed values.

2. In order that the measurement of the DCFCs be made easily and simply without the complex rigup that is used now, an attempt is made to identify a physical model that can explain the DCFCs. Further to verify this model, the variation of DCFCs with variation of cutting conditions is co-related to stable cutting data obtained under those very same cutting conditions.

In the past, as described in detail in Chapter 2, work has been concentrated in the area of obtaining the transfer function of the cutting process with various tests instituted to check the accuracy and validity of the measured or computed data. Also, since well-established theories to predict cutting stiffness under stable cutting conditions exist, many research workers have attempted to study the dynamic cutting process by either cutting at low speeds or using high speed photography. The aim of all these studies have been to form mathematical models to predict the dynamic

behaviour of certain parameters like shear plane angle, shear plane length etc. so that the theories now available to compute stable cutting forces could be used to compute dynamic cutting forces and consequently, the Dynamic Cutting Force Coefficients. However, models constructed and verified when cutting at low velocities are of doubtful authenticity since the cutting speeds in practice are extremely high in comparison to the cutting speeds used in the experiments. Also, no attempts to prove the validity of these models at higher cutting speeds have been made. The studies made, using high speed photography have only gone on to show how complex the dynamic cutting process really is.

The work presented in this thesis is therefore, a first attempt to build a physical model to explain some of the Dynamic Cutting Force Coefficients, measured using the double modulation method.

CHAPTER 2

LITERATURE SURVEY

Methods or techniques developed to obtain the transfer function of the cutting process can be broadly classified into the following groups:

2.1.1 QUASI-EXPERIMENTAL METHODS

Under the category of this classification a number of methods have been developed which are briefly described in the following pages.

Tobias and Fishwick (5) proposed that under dynamic cutting the chip thickness, the rate of penetration (i.e. variation of feed rate) and the cutting velocity undergo cyclic variations simultaneously. As a result the dynamic cutting force can be expressed in the following form:

$$F = b(k_1 ds + k_2 dr + k_3 d\Omega) \dots \dots \dots 2.1$$

where ds , dr and $d\Omega$ are variations in the uncut chip thickness, rate of penetration and rotational speed respectively. b is the width of cut and F is the dynamic cutting force.

The dynamic coefficients k_2 and k_3 were related to steady state cutting coefficients K_s and K_Ω as follows:

$$k_2 = \frac{2\pi(K_s - k_1)}{\Omega} \dots \dots \dots 2.2$$

$$k_3 = K_\Omega - \frac{K_s - k_1}{\Omega} \dots \dots \dots 2.3$$

where K_s was the coefficient, determined from the slope of the Force-feed Relationship, K_Ω the coefficient determined from the slope of the Force-speed Relationship of Stable-Cutting Experiments and k_1 being determined from dynamic cutting experiments.

K_s and K_Ω were taken as constants about the mean cutting condition. In general, the dependence of cutting force on speed was neglected and equation 2.1 was reduced to:

$$F = b[k_1(x_i - x_0) + j\omega k_2 x_i] \dots \dots \dots 2.4$$

The dependence of cutting force on speed could not be neglected; however, if the modal direction of the tool was in the direction of the cutting speed. The imaginary part depends on the velocity of tool oscillation and has the characteristics of a damping force which could assume positive or negative values assisting in stabilizing or de-stabilizing the cutting process.

Das and Tobias (6) developed a mathematical model of a regenerative cutting process where the effect of inner and outer modulation were studied independently. The term inner modulation defines the waviness of the surface being cut or wave cutting and the term outer modulation defines the waviness of the surface cut in the previous pass or wave removing. The analysis was based on the geometry of the dynamic cutting process and the expressions for steady cutting forces were modified to account for the cyclic

variation of different cutting parameters. The arguments leading to the expressions for various components of the dynamic cutting force are as follows:

The steady state cutting force is expressed by:

$$F_v = k_c b \ell \dots \dots \dots 2.5$$

$$F_p = k_c b \ell \frac{(D \cos \phi - 1)}{D \sin \phi} \dots \dots \dots 2.6$$

where b = chip width

k_c = the slope of F_v and shear plane area

ϕ = shear plane angle

ℓ = length of shear plane

D = Universal Machinability Index

For wave cutting the instantaneous shear plane length is given by the equation:

$$\ell_s = \frac{s + ds \sin \omega t}{\sin \phi} \dots \dots \dots 2.7$$

For wave removing the instantaneous shear plane length is given by the equation:

$$\ell_s = \frac{ds(\sin \omega t + \delta_0)}{\sin \phi} \dots \dots \dots 2.8$$

where s is the nominal depth or feed rate and ds is the variation in depth of cut due to tool vibration and δ_0 is the phase angle between the shear plane length variation and the uncut chip thickness.

Substitution of equations 2.7 and 2.8 into equations 2.5 and 2.6 gives the total static and dynamic parts of the

cutting force components along and perpendicular to the instantaneous direction of cutting for inner and outer modulation. Only the dynamic parts are considered and they are as given below:

$$F_v = dF_{co} \sin(\omega t + \delta_{vi}) \dots \dots \dots 2.9$$

$$F_p = dF_{to} \sin(\omega t + \delta_{pi}) \dots \dots \dots 2.10$$

$$F_v = K_{\ell c} ds(\sin \omega t + \delta_o) \dots \dots \dots 2.11$$

$$F_p = K_{\ell t} ds(\sin \omega t + \delta_o) \dots \dots \dots 2.12$$

where the terms dF_{co} , dF_{to} , $K_{\ell c}$, and $K_{\ell t}$ are functions of D , ϕ , s , ω , v , and k_c .

This analysis is; however, based on assumptions which have been later proven as doubtful. The important point of this work; however, is the indication of the independent behaviour of the inner and outer modulations. It was also shown that by combining the individual equations of the two modulations, the total dynamic force could be computed.

Nigm, Sadek, and Tobias (7) further refined the earlier model of Das and Tobias (6), the development being based on dimensional analysis of steady state cutting data which forms the basis of the dynamic theory. This amounted to the introduction of dimensionless groups characterizing strain rate and temperature effects to derive explicitly the dependance of the chip thickness ratio in terms of cutting parameters α the rake angle, s the feed rate, and v the cutt-

ing velocity. Though much better correlation of experimental and computed results were achieved than before, the method is extremely complex especially where the theoretical aspect of the work is concerned.

Peters and Vanherck (8) used the stability equation (2.13) proposed by Flusty (1) to predict a limit width of cut b_{lim} .

$$b_{lim} = \frac{1}{2rG_{min}} \dots \dots \dots 2.13$$

These authors proposed the use of the incremental cutting stiffness k_i instead of the dynamic cutting coefficient r . The values of k_i were determined from static cutting experiments. The ratio of incremental cutting force ΔF to the increment in chip thickness was determined separately for the main and thrust cutting forces. Thus, the values of k_i were determined for various cutting conditions and b_{lim} predicted for a single degree of freedom structure whose G_{min} (minimum of the real part of the frequency response curve) was known. The predicted and the experimentally determined values of b_{lim} for the given rig showed a reasonable correspondence though similar experiments performed at Eindhoven (9) showed large discrepancies. In any case this technique was inadequate to study the dynamic cutting process in detail.

2.2 EXPERIMENTAL METHODS

Procedures devised under this category can be further classified into two types.

2.2.1 STIFFNESS METHODS

Kals (9) proposed that the cutting process adds stiffness and damping to the total machining system over that available from the machine tool structure. Thus, he represented the total machining system as shown in Figure 2.

In Figure 2, K and C represent stiffness and damping of the machine tool structure and K_c and C_c , the corresponding quantities due to the cutting process. The analysis was oriented to obtain K_c and C_c from the pulse responses of the machine tool while idling and while cutting. In actual practice, a single degree of freedom system was used, whose compliance in its modal direction was much higher than that of the machine tool. From the measurement of frequency and damping ratio of the measured pulse responses, the values of K_c and C_c were computed by vectorial subtraction of stiffness and damping values obtained for the two cases. This method is extremely simple though only the inner modulation behaviour can be studied as the pulse response data can be taken for only one revolution while the outer surface of the chip is kept free of any modulation to eliminate the effect of regeneration. The values of K_c and C_c obtained by this method in

fact represent the Real and Imaginary Components of the Dynamic Cutting Force Coefficients for Inner Modulation. The results of these investigations showed beyond doubt that the cutting process exhibits damping which varies significantly with the cutting speed and under certain conditions, where the cutting process exhibits least stability, was shown to be even negative.

The above method is in general, the stiffness method. Van Brussel and Vanherck (10) further developed the stiffness method by devising an experimental technique to control the phase shift between inner and outer modulation. Thus, the effect of the two modulations could be studied separately. The following force equations were applied for both sides of the modulated chip:

$$F_i e^{j(\omega t + \delta_i)} = x_i e^{j\omega t} (R_i + jI_i) b \dots \dots \dots 2.14$$

$$F_o e^{j(\omega t + \delta_o + \epsilon)} = x_o e^{j(\omega t + \epsilon)} (R_o + jI_o) b \dots \dots \dots 2.15$$

where

Index 'i' refers to the inner modulation

Index 'o' refers to the outer modulation

δ_i and δ_o are phase shift of dynamic cutting force components with respect to inner and outer modulations

x_i and x_o respectively

ϵ is the phase shift between the two modulations.

The cutting process stiffness was then experimentally

determined using the stiffness method described earlier. The cutting coefficients R_i , I_i , R_o and I_o were computed from equation 2.14 and 2.15, from the experimental data of cutting stiffness F/x for two separate values of phase shift ϵ . The cutting coefficients, thus obtained refer to the modal direction of the test rig. In order to obtain the Dynamic Cutting Force Coefficients for the main cutting force and the thrust force, the experiment was repeated using two test rigs having a different modal direction.

Cutting coefficients were determined for different cutting conditions of feed and speed and their effects on various components of Dynamic Cutting Force Coefficients were established. The effects were found to be very similar as observed by Kals (9).

2.2.2 DYNAMOMETER METHODS

The following can be classified under the category of dynamometer methods.

Opitz and Werntze (11) devised an experimental technique to measure the dynamic cutting force coefficients using a two component cutting force dynamometer and a capacitive probe to measure tool displacement. The cutting was performed while the tool was excited at a certain frequency, the tool representing a single degree system.

The signals of cutting force and tool displacement were recorded in a process control computer and were further

processed digitally to obtain Dynamic Coefficients, chip thickness variation, phase difference between the cutting force components and chip thickness and the phase shift between inner and outer modulations. These authors gave the values of Dynamic Cutting Force Coefficients as a ratio of cutting force component to the chip thickness variation together with the phase shift between these quantities. Their experimental set-up did not allow any control over the phase relation between inner and outer modulation. However it was reported that this phase shift did not change significantly for the period for which the signals were recorded. This phase shift was however, measured by comparing signals of tool displacement at the current revolution of the workpiece and that during the previous revolution. The coordination of the tool displacement signals for the two consecutive revolutions was made possible by using a shaft encoder mounted at the end of the lathe spindle to control the digitization process for each revolution.

The tests were conducted for various cutting conditions and the effect of the phase shift ' ϵ ' between inner and outer modulation was also investigated. It was concluded that the main cutting force leads, slightly, the chip thickness variation and was constant over the whole range of ' ϵ ' while considerable change was observed in the phase shift of

the thrust cutting force. A significant variation of the Dynamic Cutting Force Coefficient was observed as the cutting speed was varied. These coefficients were found to have little variation with variation of feed rate or excitation frequency.

Goel and Tlustý (2,3,4) developed the double modulation method which overcomes drawbacks encountered in all other methods. It is a dynamometer method and, since it was utilized extensively in this work, is described more in detail in the following chapters.

2.3 OTHER INVESTIGATIONS ON THE DYNAMIC CUTTING PROCESS

Almost all the methods developed to quantify the transfer function of the cutting process have been explained in the preceding pages. However a number of workers have tried to study the dynamic cutting process using high speed photography. This may have been attempted to basically develop theoretical models which can predict certain cutting parameters like shear angle variation etc., after which the transfer function of the cutting process can be obtained by using already available static cutting data.

MacManus and Pearce (12) studied the dynamic behaviour of the effective shear angle and tool chip contact length during wave removal using the high speed photographic technique. They found that the amplitude of the varying shear angle was

frequency sensitive, i.e. increase in frequency led to increase in the amplitude of variation of the shear angle. The phase angle between the varying shear angle and varying chip thickness was also frequency sensitive. It was found to be, with increasing frequencies, increasingly lagging at low frequencies and decreasingly leading at high frequencies.

The tool chip contact length was also studied. At lower frequencies, less than 200 Hz, the contact length was seen to vary in phase with uncut chip thickness and its peak to peak amplitude proved sensibly constant with a condition of dynamically constant specific contact length i.e. the fractional variation of contact length was compatible with that of the uncut chip thickness. At higher frequencies; however, it was observed that a progressive reduction in the peak to peak amplitude of contact length occurred with increasing frequency, in spite of constant variation of uncut chip thickness implying that at higher frequencies the specific contact length was dynamically invariant. A theoretical model was also proposed and under the conditions reported, produced satisfactory correlation between computed and measured results, thus offering the prospect of predictability. However this work was not extended to predict the transfer function of the cutting process by the authors.

Sarnicola and Boothroyd (13,14) undertook a study of the dynamic response of the shear angle in wave removing (13) and later on in wave cutting and regeneration (14). In wave removing experiments they scribed striations perpendicular to the cutting direction on the side of each specimen at known intervals, starting at the peak of each wave. The variation of shear angle during wave removing was measured from the distortion of these striations, after a cut was taken. Cutting forces were also measured and a theoretical model was built which predicted fairly accurately the shear plane angle and the dynamic force components in wave removing.

In wave cutting and regeneration experiments (14), a photographic technique was used and a model built to predict the response of the shear angle only. Reasonably good correlation was achieved but no attempt to compute the dynamic force components was undertaken. However in all these experiments the material used was 90/10 brass and the cutting speeds used were extremely small in comparison to what is normally encountered in practice.

It is of interest to note here, that these authors attempted to evaluate the contention of other research workers that fluctuations in clearance angle might have an effect on tool forces during wave generating. The range of clearance angles experimented with was all in the positive range from +2 to +10 degrees and the conclusion drawn was

that fluctuations in clearance angle had no effect at all on the force components.

Stewart and Brown (15) studied regenerative chatter using high speed photography and observed that the coefficient of friction μ fluctuates dynamically as a function of the instantaneous shear plane angle ϕ_i , instantaneous shear plane length L_{si} and instantaneous rake angle α_i . A mathematical model relating the above mentioned parameters was first formulated using a thin shear plane model and assuming that the resultant forces on the shear plane and rake face are equal, opposite and colinear. Force and moment equilibriums were considered in formulation of the equations. Experimental results verified the above formulated mathematical model. However the work does not extend to compute the transfer function of the cutting process.

Ramaswami, Van Brussel, and Vanherck (16) made a study of the dynamic machining characteristics of Free Machining Steel. They observed that the Dynamic Cutting Force Coefficients for Free Machining Steel, measured using a dynamometer method, were smaller in all cases than those for Plain Carbon Steels. They computed the stability limit using these measured DCFCs for the CIRP test rig and later experimentally verified the same and found good agreement. They also observed a characteristic minimum for Free Machining Steels as in the case of other types of steels,

though the cutting speed at which this occurred for Free Machining Steels was generally higher than the speed at which a characteristic minimum occurred for Plain Carbon Steels. They also observed no Built-Up-Edge formation when cutting Free Machining Steels even at low speeds (200 ft/min) but the existence of a characteristic minimum stability limit around 300 ft/min, leading to the conclusion that the contention of some research workers that the characteristic minimum could be associated with formation of the Built-Up-Edge, to be incorrect.

CHAPTER 3
THEORETICAL BACKGROUND, EXPERIMENTAL EQUIPMENT
AND TECHNIQUE

The material discussed in this chapter and pertaining specially to the measurement of the Dynamic Cutting Force Coefficient is more extensively covered by Goel (2). However all that is relevant to the scope of work of this thesis, including modifications of the experimental rig is covered briefly in this chapter.

3.1. THEORETICAL BACKGROUND OF THE MEASUREMENT OF
DYNAMIC CUTTING FORCE COEFFICIENTS

The regenerative cutting process is analysed on the assumption that the inner and outer modulations behave independently and that the dynamic cutting forces are related separately to the two modulations.

Therefore we have for the individual components:

$$F_i = bX_i A \dots\dots\dots 3.1$$

and $F_o = bX_o B \dots\dots\dots 3.2$

where the subscript i refers to the inner modulation or wave cutting and the subscript o refers to the outer modulation or wave removing and A and B are the corresponding DCFCs.

The total force can then be written as:

$$F = F_i - F_o = b(X_i A - X_o B) \dots\dots\dots 3.3$$

In the present work, only two components of forces were relevant as orthogonal cutting was adopted. The total dynamic force in the two directions can then be written as

$$F_p = b(X_i A_p - X_o B_p) \dots \dots \dots 3.4$$

for the thrust direction and

$$F_v = b(X_i A_v - X_o B_v) \dots \dots \dots 3.5$$

in the main cutting force direction.

Now considering only the thrust component represented by equation 3.4. To evaluate the coefficients A_p and B_p , at least two equations with different phase shifts between the two modulations X_o and X_i are necessary.

Thus,

$$F_{p1} = b(X_{i1} A_p - X_{o1} B_p) \dots \dots \dots 3.6$$

$$F_{p2} = b(X_{i2} A_p - X_{o2} B_p) \dots \dots \dots 3.7$$

Solving of A_p and B_p , we get:

$$A_p = \frac{\frac{F_{p1}}{X_{o1}} - \frac{F_{p2}}{X_{o2}}}{\frac{X_{i1}}{X_{o1}} - \frac{X_{i2}}{X_{o2}}} \cdot \frac{1}{b} \dots \dots \dots 3.8$$

and

$$B_p = \frac{\frac{F_{p1}}{X_{i1}} - \frac{F_{p2}}{X_{i2}}}{\frac{X_{o2}}{X_{i2}} - \frac{X_{o1}}{X_{i1}}} \cdot \frac{1}{b} \dots \dots \dots 3.9$$

By virtue of the design of the test rig it is possible to know the exact phase shift between the inner and

outer modulations X_i and X_o . Furthermore, the phase shift is maintained constant throughout the period of cutting.

Therefore, the following relations are valid:

$$\frac{X_{i1}}{X_{o1}} = e^{j\epsilon_1} \dots \dots \dots 3.10$$

and

$$\frac{X_{i2}}{X_{o2}} = e^{j\epsilon_2} \dots \dots \dots 3.11$$

Substituting the above equations 3.8 and 3.9 reduce to:

$$A_p = \frac{\frac{F_{p1}}{X_{i1}} e^{j\epsilon_1} - \frac{F_{p2}}{X_{i2}} e^{j\epsilon_2}}{e^{j\epsilon_1} - e^{j\epsilon_2}} \cdot \frac{1}{b} \dots \dots \dots 3.12$$

$$B_p = \frac{\frac{F_{p1}}{X_{i1}} - \frac{F_{p2}}{X_{i2}}}{e^{-j\epsilon_2} - e^{-j\epsilon_1}} \cdot \frac{1}{b} \dots \dots \dots 3.13$$

Similarly the coefficients for the vertical components of force can be written as:

$$A_v = \frac{\frac{F_{v1}}{X_{i1}} e^{j\epsilon_1} - \frac{F_{v2}}{X_{i2}} e^{j\epsilon_2}}{e^{j\epsilon_1} - e^{j\epsilon_2}} \cdot \frac{1}{b} \dots \dots \dots 3.14$$

and

$$B_v = \frac{\frac{F_{v1}}{X_{i1}} - \frac{F_{v2}}{X_{i2}}}{e^{-j\epsilon_2} - e^{-j\epsilon_1}} \cdot \frac{1}{b} \dots \dots \dots 3.15$$

All the terms on the RHS of equations 3.12 to 3.15, except for the phase angles ϵ_1 and ϵ_2 , are harmonically varying quantities and have a real and imaginary component. Consequently, the dynamic coefficients A_p , B_p , A_v and B_v

have real and imaginary components.

3.2 EXPERIMENTAL EQUIPMENT

The equipment used can be classified into two categories, owing to the nature of the conditions under which the cutting was carried out.

3.2.1 DYNAMIC CUTTING

The set-up for the measurement of the dynamic forces and displacements required to compute the Dynamic Cutting Force Coefficients as per equations 3.12 to 3.15 are shown in Figure 3 and Figure 4.

The test rig consists of a single degree of freedom system on which a two component cutting force tool dynamometer is mounted. The dynamometer is capable of measuring the cutting force components in the thrust force direction and the main cutting force direction using piezo-electric force transducers. The charge generated in the piezo-electric crystals is fed into their respective charge amplifiers to give voltage signals corresponding to the forces.

The thrust force signal then undergoes two compensations. The first is for cross sensitivity. It was found that owing to the construction of the dynamometer a dynamic force in the direction of the main cutting force resulted in

a signal in the thrust force direction transducer. This signal was proportional to the magnitude of the former and 180° out of phase with it. To eliminate this cross sensitivity signal, a parallel output was tapped from the main cutting force signal, so as to not affect it, attenuated to match the cross sensitivity signal in amplitude and then added to it in the adding circuit shown in Figure 5. Since the two signals were 180° out of phase, they cancelled each other and eliminated the cross sensitivity signal.

The construction of the dynamometer ensured that there was no appreciable output signal in the main cutting force direction transducer while the dynamometer was subjected to a dynamic load purely in the thrust force direction. With this arrangement all dynamic cross sensitivities at the operating frequencies were less than 2%.

The introduction of this compensation for cross-sensitivity was the only major addition to the experimental rig as designed by Goel (2). This was directly the result of the increase in the overhang of the cutting tool on the dynamometer in the horizontal direction. This change in design of the dynamometer resulted from the change instituted in the feed direction from longitudinal feed to cross or radial feed. The longitudinal feed direction required the manufacture of thin tubes resulting in not only tedious work but also an extensive waste of workpiece material.

The thrust force signal was then compensated for inertia force by subtracting from it the inertia force signal obtained by an accelerometer mounted in the direction of the thrust force. This is done by feeding the two signals into an Inertia Force Compensation Circuit. The tool displacement is measured with the use of a capacitance probe, the signal from which is fed into a Wayne-Kerr capacitance bridge. The bridge gives out a voltage signal proportional to the displacement. The force signals and the displacement signal are fed into the Hewlett-Packard Fourier Analyser System which consists of the following:

1. HP5465A Analog to digital converter
2. HP5475A Control Unit
3. HP2100A Computer
4. HP5460A Display Unit.

The system is also equipped with various I/O devices. The system takes in the data to carry out the analysis as explained further on.

The cutting tool is excited by an electro-hydraulic exciter, powered by a 3000 psi hydraulic power pack and controlled by a servo-valve drive amplifier. The frequency of excitation is linked to the rotational speed of the lathe spindle to control and maintain the phase shift between inner and outer modulation. This is achieved as follows:

The pulses generated by a digitizer mounted at the

end of the lathe spindle are divided by a certain integer in the frequency divider the number being set on the frequency divider by thumb wheel switches. This integer number determines the actual frequency of excitation in combination with the spindle speed and independently by the phase shift ϵ between the inner and outer modulation. The divided pulses are then shaped into a sine wave by passing them through a pulse shaper and a low pass filter which filters out the higher harmonics. The almost sinusoidal signal from the low-pass filter is further amplified by the servo-valve drive amplifier which controls the amplitude of the exciting force of the electro-hydraulic exciter.

3.2.2 , STABLE CUTTING

The set-up used for measuring stable cutting data is shown in Figure 6. Since the experiments consisted of measuring the two components of cutting forces at various cutting speeds the same dynamometer used for dynamic measurements was used. The cross-sensitivity compensation had to be re-adjusted for static loading conditions, the output after attenuation being connected to a four channel pen type recorder.

Carbide inserts with various types of clearance angles were used in stable cutting experiments for reasons explained and discussed in Chapter 4.

3.3 EXPERIMENTAL TECHNIQUES

These can also be classified into two categories.

3.3.1 DYNAMIC CUTTING

The Analog to Digital converter has only two channels; hence, experiments have to be repeated to analyse the two force directions separately.

The following parameters are then set on the AD converter:

1. Block size
2. Frequency resolution, total record time, time resolution and total frequency; the above mentioned parameters being inter-related.

The Fourier Analyser system is then key board programmed to do the following steps:

1. Take in four samples of force and displacement signals.
2. Fourier Analyse all the above signals.
3. Print out the magnitude of these signals at and close to the operating frequency in real and imaginary form.
4. Compute and print out the ratio of force/displacement for the four samples. Since the samples were all taken at near identical conditions, their ratios should

fairly equal. This is just to check the accuracy of the recorded data.

The cutting conditions are then selected. The frequency divider is set to give the required frequency and phase angle between the two modulations. The rotational speed may have to be slightly adjusted to give the correct frequency and the required phase shift, the adjusting normally affecting the cutting speed to the extent of 2 to 3%. The hydraulic supply is pressurized and the servo-valve amplifier set to give the required amplitude of vibration. Cutting is commenced by engaging the feed lever of the lathe and the Fourier Analyser System commanded to record the signals. Once the recording of the signals is completed, the cutting is stopped and other computations as explained earlier are carried out. If the measurement is being carried out in the thrust force direction the Inertia Compensation may have to be checked and set.

This procedure is repeated for another phase shift between inner and outer modulations and the magnitudes of force and displacement printed out on the teletype. This data is then processed on the CDC 6400 computer to obtain the Dynamic Cutting Force Coefficients as per equations 3.12 to 3.15. Since four samples of data are taken for each phase angle, a minimum of sixteen values of DCFCs are computed if experiments are carried out for two phase angles

only. Normally, data was collected for a minimum of three phase angles, the average value of the sixteen values obtained for each pair of phase angles being plotted to check for dispersion and accuracy.

This procedure is repeated for different materials, different cutting speeds and different tool wear conditions as explained and discussed in Chapter 4.

3.3.2 STABLE CUTTING

The procedure here consists of selecting the right cutting conditions, the right cutting tool and recording the two force signals simultaneously on the multi-channel pen-type recorder during cutting. The cross sensitivity compensation will have to be checked and adjusted for static loading before commencing the tests.

CHAPTER 4

RESULTS AND DISCUSSIONS

The results and the discussions are presented in this chapter in accordance with the two main objectives of work outlined in Chapter 1.

4.1 VERIFICATION OF THE VALIDITY OF THE MEASURED DYNAMIC CUTTING FORCE COEFFICIENTS

Using the experimental system described in Chapter 3, the Dynamic Cutting Force Coefficients were measured for the steels given in Table 4.1.

The cutting tool and insert used are described below.

INSERT - Sintered Carbide (Kenametal Grade K20)

TOOL - Rake angle $\alpha = 3^\circ$

Clearance angle $\gamma = 7^\circ$

The cutting conditions used for this objective are those normally encountered in practice and are as given.

CUTTING SPEED - 50, 100, 200, 300, 400, 500, 600

v(ft/min)

FEED RATE - 0.0051

s(in/rev)

FREQUENCY - 200

f(Hz)

FLANK WEAR - 0 - 0.002

V_B (in)

Table 4.1 WORKPIECE MATERIALS

WORKPIECE MATERIAL	BRINELL HARDNESS NO. (B.H.N.)	YIELD STRENGTH (PSI)	CHEMICAL COMPOSITION %									
			C	Mn	P	S	Si	Ni	Cr	Mo		
1020 Steel	118	48,500	0.20	0.45	0.04	0.04	0.05					
1045 Steel	170	54,250	0.45	0.70	0.04	0.04	0.05					
4340 Steel	270	68,500	0.40	0.75	0.04	0.04	0.04	0.275	1.82	0.8	0.25	

5

The flank wear used in these experiments was controlled to simulate a sharp tool condition. This is however, not encountered in practice for any length of time, but was adopted for this section of objectives for the following reasons:

a) Since the objective was to compare the theoretically computed b_{lim} from the measured DCFCs to the actually obtained b_{lim} on a certain machine tool, if b_{lim} tests were conducted with the same controlled condition of tool wear, the tests would be comparable and valid.


b) : It had been found earlier by Goel (2) and Tlustý, Moriwaki and Goel (4) that the DCFCs do not change appreciably with change in frequency when cutting with an unworn tool but change appreciably with change in frequency when cutting with a worn tool. The DCFCs were measured at an excitation frequency of 200 Hz owing to the fact that the best harmonic excitation signal was obtained on the rig at that frequency. The b_{lim} tests were conducted on a lathe which was later found to have a chatter frequency in the range of 90 to 130 Hz depending on the workpiece size. To accommodate this rather large variety of frequencies without affecting the validity of the results, these tests had to be conducted with an unworn tool. If tests had been conducted with a worn tool, this variety of frequencies would have resulted in large differences of the actual DCFCs from

the measured DCFCs, thus making any comparison illogical.

The measured DCFCs are shown in Figure 7 to Figure 12. The relevant cutting conditions, etc. are shown on the graphs. The plotted points are the average DCFC values obtained for different sets of phase differences, three sets being the minimum. The scatter of these values was found to be consistently small except at the very low cutting speed of 50 ft/min.

The dynamic characteristics of the TOS SN 40-B lathe was measured using the Impact Testing Technique. Hammer blows were given to the workpiece at the tailstock end in the horizontal and vertical directions. The relative vibration between the workpiece and the toolpost was measured in the horizontal direction only, by a displacement transducer. The impact force signal, measured by an impact transducer attached to the hammer, and the amplitude signal were both fed into the Fourier Analyser System. The Fourier Analyser was programmed to Fourier Analyse both the signals and obtain the real and imaginary components of the frequency response curve of the Machine Tool System. A ten times averaging was done. The horizontal hammer blow gave the direct receptance and the vertical hammer blow gave the cross receptance. Both receptances as plotted out by the Fourier Analyser are shown on Figures 13 and 14.

Using the values of the measured DCFCs and the



measured receptances of the lathe, the limit chip, or b_{lim} as it is commonly known, was computed. The equations and the computer program used are described and listed in the Appendix. The computed values for the three materials, 1020, 1045 and 4340 steels are plotted in dashed lines in Figures 15, 16, and 17.

B_{lim} tests were then conducted on the TOS SN 40-B lathe under the same conditions of tool wear, feed rate and speeds as used in the measurement of DCFCs. The tool used had a 90° SECA and the rake angle was $\alpha = 3^\circ$. Workpiece dimensions were kept as close as possible to the dimensions of the workpiece which was mounted on the lathe during the measurement of the frequency response. Cutting was carried out at the tailstock end only. The measured values of b_{lim} just before chatter occurred, are plotted in full lines on Figures 15, 16, and 17 for comparison.

It can be seen from these figures that extremely good correlation was obtained under most conditions. The computed values were lower than actual values at very low cutting speeds of around 50 ft/min. However at speeds normally used in general manufacturing the predicted values almost coincided with actual values. It had been observed earlier that at low cutting speeds the values of DCFCs measured were not very reliable owing to a larger extent of scatter. This could probably explain the discrepancy between

the measured and computed b_{lim} values at low speeds. At low cutting speeds the cutting process is highly irregular and not smooth; thus; leading to errors in force measurements.

These tests clearly satisfy the first objective of this work, that the Dynamic Cutting Force Coefficients as measured by the Double Modulation Method does indeed represent the transfer function of the cutting process, accurately, and could be used in conjunction with dynamic characteristics of the machine tool to predict the limit of stability.

4.2 CORRELATION OF THE DYNAMIC CUTTING FORCE COEFFICIENT WITH STABLE CUTTING FORCES

The purposes of this objective, as explained in Chapter 1 earlier, is to develop a suitable correlation between the Dynamic Cutting Force Coefficients and stable cutting forces so that the DCFCs could then be easily computed or arrived at from the measurement of these stable cutting forces. All the special instrumentation that goes into the measurement of the DCFCs could be then avoided. In the process of achieving this, the dynamic cutting process could be analysed also. In this work, only two of the DCFCs in each component of force are analysed. They are the real and imaginary components of the inner modulation for the

forces in the main cutting force and thrust directions.

In Figure 18, block C represents a tool with a certain amount of flank wear in the process of wave cutting. The motion of the tool is assumed to be harmonic. If this process is carefully analysed, the following becomes obvious.

When the tool is at point 'a', the wear land on the tool is co-incident with the surface being cut. At this position the tool can be pictured to be cutting with a zero degree clearance angle. From point 'a' to point 'c' through point 'b', because of the nature of the slope, the cutting edge can be pictured to be cutting with a negative clearance angle, or in other words, the lower edge of the flank wear would be interfering with the surface just exposed by the tool. The maximum interference would occur at point 'b' where the slope is maximum the interference increasing from point 'a' to point 'b' and then reducing from point 'b' to point 'c'. At point 'c' the condition of zero degree clearance would occur. Now from point 'c' up to point 'e' through point 'd', the tool can be pictured to be cutting with a +ve clearance angle, the angle being maximum at point 'd', the point of greatest slope, and as before, the angle increasing from point 'c' to point 'd' and decreasing from point 'd' to point 'e'.

Block B shows the variation of the cutting force along the length of the cut. This force variation is basically owing to the change in chip thickness and is maximum when chip thickness is maximum, i.e. at point 'c' and minimum when chip thickness is minimum, i.e. at points 'a' and 'e'.

This variation in force is obviously in phase with the vibration amplitude and would therefore, constitute the real part of the Dynamic Cutting Force Coefficient for inner modulation.

An exploratory investigation was conducted to find out if changing clearance angles gave changing forces. A sharp insert was used to simulate a positive clearance angle. In the positive clearance angle region the variation of the angle had no effect on the forces, as obtained by Sarnicola and Boothroyd (14). A normal worn insert as shown in Figure 19 was used to simulate 0° clearance angle and inserts worn out as shown in Figure 20 were used to simulate negative clearance angles. Initially tools were worn out by actual cutting but later on since no appreciable difference was observed in these measurements and measurements made with artificially worn tools, the latter was adopted. The exploratory investigation revealed a difference in both the main and thrust forces when cutting with tool tips with the different types of clearance angles. It also revealed that forces when cutting with negative clearance angles was generally higher than when cutting with 0° clearance angles and forces when cutting with positive clearance angles were generally lower than when cutting with 0° clearance angles.

Coming back to Figure 18, block B, if the harmonic force generated in phase with the vibration could be found

equivalent to the force that would be generated in stable cutting by an insert with 0° clearance angle, then the variation of clearance angle would give rise to another vibratory force 90° out of phase with the vibration. This would then be the damping force and its generation is explained below.

Observing block A and block C, at point 'a', no additional damping force would be generated as the clearance angle is 0° at this point. However, by the time the cutting edge reaches point 'b', the slope and hence, the interference is maximum, so the damping force is also maximum. At point 'c', since the slope reduces to 0° , the damping force also reduces to zero. From point 'c' to point 'e' through point 'd', the cutting edge cuts with a positive clearance, thus causing the damping force to assume a level less than the mean value or in other words, a negative nature. The assumption that the negative force from point 'c' up to point 'e' is sinusoidal, is obviously incorrect since variation of clearance angles in the positive range have been found to have no appreciable affect on the forces, but it is maintained so for simplicity at the present. After point 'e', the cycle repeats itself.

The reason to justify calling this variable force component as the damping force is explained below. When the tool is penetrating into the material from point 'a' to point 'c' (studying blocks A and C), this force assumes

a magnitude which opposes the velocity of the tool into the material and is maximum at point 'b' when the velocity is maximum. From point 'c' to point 'e' the tool pulls out of the material or has negative velocity; the force generated is negative in nature, thus opposing the pulling out of the tool. This reaches a negative maximum at point 'd' when the tool has a maximum negative velocity. Thus in effect this force opposes the vibratory motion and acts in phase with the velocity of the tool and hence, can be justifiably called a damping force or the imaginary component of inner modulation.

Based on this physical model and encouraging results of the exploratory investigations, stable cutting tests were conducted using cutting edges with various clearance angles for three materials. Earlier the Dynamic Cutting Force Coefficients had been measured for these materials at conditions which were all similar to the conditions used for measurements conducted for the first objective, except for one. The cutting tool edge used for the measurement of the DCFCs had a flank wear land width of 0.003" to 0.005" generated by actual cutting. The materials investigated were 1045 steel, 4340 steel and stainless steel 304, the composition and properties of which is given below. Properties and chemical compositions of 1045 and 4340 steel are given in Table 4.1.

CHEMICAL COMPOSITION :

WORKPIECE MATERIAL NO.	BRINELL HARDNESS (B.H.N.)	YIELD STRENGTH (PSI)	C	Mn	P	S	Si	Ni	Cr
SS304	149	42,000	.08	2.0	0.045	0.030	1.0	8-10.5	20

Figures 21 to 23 show the measured stable cutting forces in the two force directions for the materials mentioned earlier. The points illustrated on the graph are the average of three or more recordings. The scatter in all cases was found to be small. The following relevant observations can be made from the graphs.

At most cutting speeds and for all the three materials investigated the cutting forces were largest in the case of the negative clearance angle. The force generated with a 0° clearance angle cutting edge was next in descending order and the sharp cutting edge or the cutting edge with the positive clearance angle generated the lowest cutting force. Tests were also conducted at certain cutting speeds for all materials with cutting edges with two values of negative clearance angles as illustrated in Figure 20. An approximate linear relationship between the change of cutting force and change in the magnitude of the negative

clearance angle was observed to exist.

There were, however, exceptions to the observation of the magnitude of cutting forces for the three different types of clearance angles at certain cutting speeds. At these speeds normally at 200 ft/min and 300 ft/min, the trend was reversed and it was found that the negative clearance cutting edge generated a lesser force than the 0° clearance angle cutting edge. For 4340 steel, Figure 22, at 200 ft/min, the cutting edge with the positive clearance generated the largest cutting force. This observation when applied back to Figure 18, block A can explain negative damping, which exists at those cutting speeds. That is, at those particular cutting speeds the damping force instead of opposing the velocity of the tool, as explained earlier, assists it, resulting in an increase in vibratory motion.

From the observations and discussions contained in the chapter , Figure 24 can be formulated. Based on this figure mathematical relationships are derived to correlate the stable cutting forces and the DCFCs. The figure is explained below.

The cutting force, f_v or f_p (main cutting force or thrust force) is represented on the Y-axis while the clearance angle is represented on the X-axis. The subscript to the symbol f or Δf signifies the clearance angle of the cutting edge to which the force plotted above corresponds. The

figure represents the most usual case, the value of Δf_{-ve} or Δf_{+ve} may in some cases be zero or assume values of the opposite nature as already discussed previously.

Based on the discussions presented earlier, the real part of the cutting force coefficient for inner modulation is given by the equation:

$$R_e(A) = \frac{f_o}{b \times s \times 2240} T/in^2 \dots \dots \dots 4.1$$

where b = width of cut (in)

s = feed rate (in/rev)

This equation can be directly applied and the results, are plotted on Figures 25 to 30. The derivation of a formula to obtain the imaginary component is a little more complex.

Change of forces generated during the cycle when the clearance angle changes from 0° to +ve is neglected in this analysis since they appear to be static in behaviour. The observation that their value does not vary with the change in the clearance angle indicates that they act only as a DC shift and are not harmonic in nature. Therefore, only the imaginary component of inner modulation generated when the clearance angle changes from 0° to negative, is considered. However, since the force is dependent on the slope of the modulation and consequently, the maximum value on the maximum slope, the value of the maximum slope has to be determined.

Assuming harmonic motion of the cutting tool in generating the modulation, the amplitude at any given instant is given by the equation:

$$X = A \sin 2\pi \frac{x}{w} \dots \dots \dots 4.2$$

where

X = amplitude (in)

A = Max amplitude (in)

x = distance along the modulation (in)

and w = wave length of the modulation (in)

$$\therefore \text{max slope is } \frac{dX}{dx} = \frac{2\pi}{w} A \cos \frac{2\pi}{w} x$$

The max slope is when $\cos \frac{2\pi}{w} x = 1$

$$\therefore \text{max slope is } \frac{2\pi A}{w} \text{ (radians)} \dots \dots \dots 4.3$$

$$\text{Now } w = \frac{V}{f} \times \frac{12}{60} = \frac{V}{5f} \dots \dots \dots 4.4$$

where

V = cutting speed (ft/min)

f = frequency (Hz)

Substituting equation A.5 in A.4

$$\text{max slope} = \frac{10\pi Af}{V} \text{ (radians)} \dots \dots \dots 4.5$$

Assuming, as mentioned earlier, that the maximum force generated in this part of the cycle is linearly proportional to the maximum slope, then

$$\text{Max Imaginary force} = \frac{\Delta f_{-3}}{3 \times \pi} \times \text{max slope}$$

$$= \frac{600 \Delta f_{-3} Af}{V} \dots \dots \dots 4.6$$

The coefficient for this part of the cycle is
 Max Imaginary Force $\times \frac{1}{A} \times \frac{1}{b} \times \frac{1}{2240} T/in^2 \dots\dots\dots 4.7$

Substituting 4.7 into 4.8, we get the imaginary coefficient

$$\frac{0.27 \Delta f_{-3} f}{V \times b} T/in^2 \dots\dots\dots 4.8$$

Equation 4.8 is divided by 2 to give the average value as this harmonic force exists for only half the cycle, giving

$$Im(A) = \frac{0.27 \Delta f_{-3} f}{V \times b} \cdot \frac{1}{2} T/in^2 \dots\dots\dots 4.9$$

Equation 4.9 can be used to compute the imaginary part of the Dynamic Cutting Force Coefficient for Inner Modulation and the values obtained are plotted on Figures 25 to 30.

A study of these figures reveal an excellent correlation in the case of both the real and imaginary values so far as the trends are concerned. The measured real parts show a greater degree of variation than the computed values. The magnitudes of the real parts are fairly similar in the case of Stainless Steel 304 with the differences varying from very small to large for the other two materials at different cutting speeds.

The computed and measured values of the imaginary component of inner modulation show a much better correlation except when the values tend to be negative. This clearly indicates that the present analysis does not explain com-

pletely the dynamic cutting process when the damping is negative. However it should be noted here that in spite of the fundamental approach adopted and the fact that this is a first attempt to explain the DCFCs, the results are encouraging.

Stable cutting force measurements were also conducted with cutting edges having clearance angles as explained before but very large flank wear land widths of about 0.010", for 1045 steel only. The DCFCs computed from this data are plotted on Figure 25 and 26 in double dashed lines. The imaginary component of the thrust coefficient is extremely large in comparison to the earlier measurement. All other coefficients increase to a lesser extent. These results are in agreement with Tlustý, Morwaki, and Goel (17).

CHAPTER 5

CONCLUSIONS

This chapter briefly compares the objectives achieved to those that were laid out in Chapter 1. Future areas of work that would find solutions to unanswered questions are also identified.

It was established conclusively that the measured Dynamic Cutting Force Coefficients do indeed represent the transfer function of the cutting process. Further, it was established, that the DCFCs could be coupled with the dynamic characteristics of the machine tool system to predict the limit of stability. This was done by comparing the experimentally obtained b_{lim} to the b_{lim} computed from the measured DCFCs and the direct and cross receptances of the machine tool system. At most speeds, specially in the range that is normally used in practice, the predicted value and the experimentally obtained value were almost coincidental. At lower speeds, large errors seemed to exist. This is probably due to the fact that at low cutting speeds the cutting process is irregular, thus affecting the force signal and consequently, the accuracy of the measured DCFCs. Work remains in this area to verify this explanation at low cutting speeds or if, some other factors influence the dynamic cutting process.

A physical model to explain the Dynamic Cutting Force Coefficients of Inner Modulation is presented. Mathematical expressions to compute these coefficients, based on the presented physical model, are derived. The Imaginary Coefficients computed from these mathematical expressions, show a good degree of agreement with the measured values except when the values become negative. The Real Coefficients computed, though having similar magnitudes as the measured values at certain cutting speeds, show a far greater degree of stability than the measured ones, which tend to change considerably with change of cutting speeds. These aspects have to be further investigated. However, if the fact, that a very fundamental approach was adopted, is considered, the degree of accuracy, with which the DCFCs have been predicted from stable cutting data, is good.

Work however, remains to find similar correlations between stable cutting forces and the DCFCs of outer modulation. Also studies have to be conducted to investigate the reasons why the magnitude of the forces change, in the manner that they do, with change of clearance angles. These studies may enable the attainment of the stage where the DCFCs could be arrived at from the basic material properties. The capability to then easily predict the limit of stability for any machine tool, under any cutting conditions and for all materials would be reached.

REFERENCES

1. Koneigsberger and Tlusty,
Machine Tool Structures, Vol. 1, Pergamon Press, 1970,
2. Goel; B. S.,
Measurement of Dynamic Cutting Force Coefficients,
Ph.D. Thesis, McMaster University, 1977.
3. Tlusty, J. and Goel, B. S.,
Measurement of the Dynamic Cutting Force Coefficient,
Proceedings of the 2nd North American Metal Working
Research Conf., 1974.
4. Tlusty, J., Moriwaki, T., and Goel, B. S.,
The Dynamic Cutting Force Coefficients for Some Carbon
Steels, Proceedings of the 4th North American Metal
Working Research Conf., 1976.
5. Tobias, S. A., and Fishwick, W.,
A Theory of Regenerative Chatter, The Engineer (London),
1958.
6. Das; M. K. and Tobias, S. A.,
The Relation between Static and Dynamic cutting of
metals, Int. Journal of Mach. Tool Des. and Res., 1971.
7. Nigm, M. M., Sadek, M. M., and Tobias, S. A.,
Prediction of Dynamic Cutting Coefficients from Steady
Cutting Data, Proceedings of Int. Mach. Tool Des. and
Res., 1971.
8. Peters, J. and Vanherck, P.,
Machine Tool Stability Tests and the incremental
stiffness, Annals of CIRP, Vol. 17, 1969.
9. Kals, H. J. J.,
Process damping in Metal Cutting, Report WT0278,
Dept. of Mech. Eng., Eindhoven University of Techno-
logy, May 1972.
10. Van Brussel, H. and Vanherck, P.,
A new method for the determination of the Dynamic
Cutting Coefficients, Int. Journal of Mach. Tool Des.
and Res., 1970.

11. Opitz, H. and Werntze, G.,
Application of a process control computer for
measurement of Dynamic Cutting Coefficients,
Laboratorium fur Werkzeugmaschinen U, Betriebslehre
Tech. Hochschule Aachen, 1972.
12. MacManus, B. R. and Pearce, D. F.,
The dynamic response of the effective shear angle on
wave removal, Proceedings of Int. Mach. Tool Des. and
Res., 1970.
13. Sarnicola, J. F. and Boothroyd, G.,
Machine Tool Chatter: Factors which influence cutting
forces during wave removing, Proceedings of the 1st
North American Metal Working Research Conference,
1973.
14. Sarnicola, J. F. and Boothroyd, G.,
Machine Tool Chatter: Effect of equivalent surface
slope on Shear Angle during Wave Generating and
Regenerative Chatter, Proceeding of the 2nd North
American Metal Working Research Conference, 1974.
15. Stewart, V. A. and Brown, R. H.,
The inter-relationship of Shear and Friction processes
in machining under Regenerative Chatter Conditions,
Proceedings of Int. Mach. Tool Des. and Res., 1971.
16. Ramaswami, R. Van Brussel, H. and Vanherck, P.,
A study of the Dynamic Machining of Free Machining
of Free Machining Steel, Proceedings of Int. Mach.
Tool Des. and Res., 1975.
17. Tlusty, J., Morwaki, T. and Goel, B. S.,
The Dynamic Cutting Force Coefficients for Some Carbon
Steels, Metalworking Research Group, Report No. 76,
McMaster University, 1976.

APPENDIX

LISTING OF COMPUTER PROGRAM TO CALCULATE
THE STABILITY LIMIT

The stability limit is calculated from the known Dynamic Cutting Force Coefficients and the horizontal direct and cross receptances of the lathe.

From the DCFCs the

$$\text{Thrust Force } F_p = b(-A_p X_i + B_p X_o) \dots \dots \dots \text{A.1}$$

and the

$$\text{Main Cutting Force } F_v = b(-A_v X_i + B_v X_o) \dots \dots \text{A.2}$$

The inner modulation X_i is then related to the forces by

$$X_i = G_1(j\omega) F_p + G_2(j\omega) F_v \dots \dots \dots \text{A.3}$$

where

$G_1(j\omega)$ is the horizontal direct receptance

and $G_2(j\omega)$ is the horizontal cross receptance

Substituting equations A.1 and A.2 in A.3 we get

$$X_i(1 + G_1(j\omega)bA_p + G_2(j\omega)bA_v) = X_o(G_1(j\omega)bB_p + G_2(j\omega)bB_v) \dots \dots \dots \text{A.4}$$

$$\text{Now limit of stability is when } \left| \frac{X_i}{X_o} \right| = 1 \dots \dots \text{A.5}$$

i.e.

$$|b(G_1(j\omega)B_p + G_2(j\omega)B_v)| = |1 + b(G_1(j\omega)A_p + G_2(j\omega)A_v)| \dots \dots \dots \text{A.6}$$

All the terms in equation A.6 are complex. The program listed multiplies all these numbers in complex form; squares the real and imaginary parts and adds them on both sides to form a quadratic equation in b , the limit of stability. The values of the DCFCs are those obtained experimentally. The values of the receptances are measured to the appropriate scale from Figures 13 and 14. Ten values of direct and cross receptances at intervals of half a cycle on either side of the frequency at which the minimum value of real part occurs on the direct receptance curve, are fed into the program. This is, since it is obvious by its magnitude, that it is the dominating mode. Limits of stability at each frequency interval is calculated.

A specimen output is also listed. This specimen corresponds to 1045 steel at 600 ft/min. The DCFCs printed on the output are taken from Figures 9 and 10. Since ten sets of values of both the direct and cross receptances are given into the program and the solution of the quadratic equation gives two roots, twenty values of b_{lim} are obtained. The lowest positive value is taken as the limit of stability which, in this case, is the circled value of 0.09608.

-3/73 TS

FTN 4.6+42E

```

PROGRAM TST(INPUT,OUTPUT,TAPE5=INPUT,TAPE6=OUTPUT)
*****
PROGRAM TO COMPUTE LIMIT OF STABILITY
*****
DIMENSION CLATURE
3P(I) THRUST COEFFICIENT FOR OUTER MODULATION
BV(I) VERTICAL COEFFICIENT FOR OUTER MODULATION
AP(I) THRUST COEFFICIENT FOR INNER MODULATION
AV(I) VERTICAL COEFFICIENT FOR INNER MODULATION
GJ1W(J) DIRECT HORIZONTAL RECEPTANCE
GJ2W(J) CROSS HORIZONTAL RECEPTANCE

DIMENSION GJ1W(100), GJ2W(100), 3P(50), BV(50), AP(50), AV(50)
COMPLEX GJ1W,GJ2W,3P,BV,AP,AV,SW,TH,UW
DATA 1.777, 1/10/
DO 3 I=1,N
READ (5,4) AP(I),3P(I),AV(I),BV(I)
WRITE (5,5)
WRITE (5,6) 3P(I),BV(I),AP(I),AV(I)
DO 3 J=1,M
IF (I.GT.1) GO TO 1
READ (5,7) GJ1W(J),GJ2W(J)
WRITE (5,8)
WRITE (5,9) GJ1W(J),GJ2W(J)
SW=(GJ1W(J)+3P(I)+GJ2W(J)+BV(I))+224J.
TH=(GJ1W(J)+AP(I)+GJ2W(J)+AV(I))+224J.
UW=CONJG(SW)
I=SW*UW
X=REAL(TH)
Y=AIMAG(TH)
X1=X*X
Y1=Y*Y
A=X1+Y1-4
B=2.*X
J=1-2-3-4.*A
IF (DET.LI.0.) GO TO 2
DET=SQRT(DET)
B1=0.5*(-B-DET)/A
B2=0.5*(-B+DET)/A
WRITE (5,10)
WRITE (5,11) B1,B2
GO TO 3
WRITE (5,12)
CONTINUE
STOP

FORMAT (8F10.5)
FORMAT (1F1,5X,^THE D.C.F.C.S.ARE^)
FORMAT (2X,^3P(I)=^,2F7.2,1X,^BV(I)=^,2F7.2,1X,^AP(I)=^,2F7.2,1X,^AV(I)=^,2F7.2)
FORMAT (4F20.10)
FORMAT (/ ,5X,^THE DIRECT RECEPTANCES ARE^).
FORMAT (3X,^GJ1W(J)=^,2E12.3,5X,^GJ2W(J)=^,2E12.3)
FORMAT (5X,^THE LIMITS OF STABILITY ARE^).
FORMAT (3X,^B1=^,F10.5,5X,^B2=^,F10.5)
FORMAT (/ ,5X,^DETERMINANT IS NEGATIVE^).
END

```

THE DIRECT RECEPTANCES ARE
 THE LIMITS OF STABILITY ARE
 B1= .37922 B2= -.17061

THE DIRECT RECEPTANCES ARE
 THE LIMITS OF STABILITY ARE
 B1= .25269 B2= -.21132

THE DIRECT RECEPTANCES ARE
 THE LIMITS OF STABILITY ARE
 B1= .21857 B2= -.25409

THE DIRECT RECEPTANCES ARE
 THE LIMITS OF STABILITY ARE
 B1= .19039 B2= -.26892

THE DIRECT RECEPTANCES ARE
 THE LIMITS OF STABILITY ARE
 B1= .11840 B2= -.26325

THE DIRECT RECEPTANCES ARE
 THE LIMITS OF STABILITY ARE
 B1= .13725 B2= -.34299

THE DIRECT RECEPTANCES ARE
 THE LIMITS OF STABILITY ARE
 B1= .11025 B2= -.45055

THE DIRECT RECEPTANCES ARE
 THE LIMITS OF STABILITY ARE
 B1= .09606 B2= -.52130

THE DIRECT RECEPTANCES ARE
 THE LIMITS OF STABILITY ARE
 B1= .10354 B2= -.60259

THE DIRECT RECEPTANCES ARE
 THE LIMITS OF STABILITY ARE
 B1= .11523 B2= -.72291

BP(I) = 56.22 BV(I) = 10.66 BV(I) = 128.44 2.27 4P(I) = -6.11 4.38 AV(I) = 91.21 2.27

GJ2W(J) = .157E-04 0.

GJ2W(J) = .160E-04 .470E-05

GJ2W(J) = .162E-04 .100E-04

GJ2W(J) = .140E-04 .136E-04

GJ2W(J) = .100E-04 .176E-04

GJ2W(J) = .680E-05 .160E-04

GJ2W(J) = 0. .170E-04

GJ2W(J) = -.60E-05 .130E-04

GJ2W(J) = -.820E-05 .640E-05

GJ2W(J) = -.780E-05 .500E-05

Material 1045
 V=600 ft/min
 s=0.0051"/rev
 VB=0-0.002"

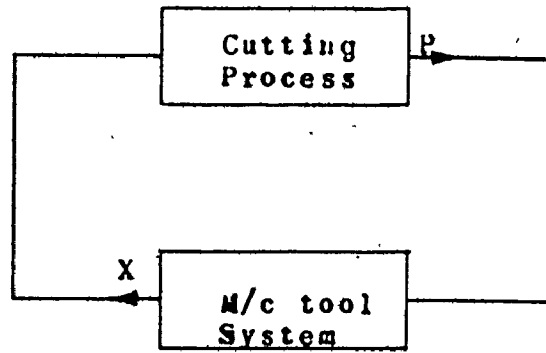


Fig. I BASIC DIAGRAM OF CHATTER

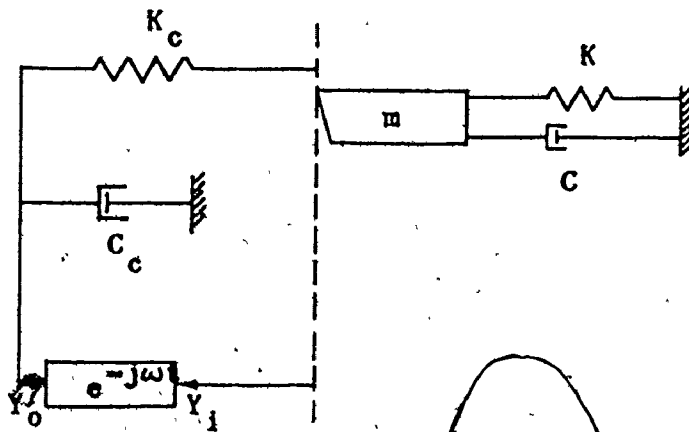


Fig. 2 KALS' CUTTING PROCESS MODEL

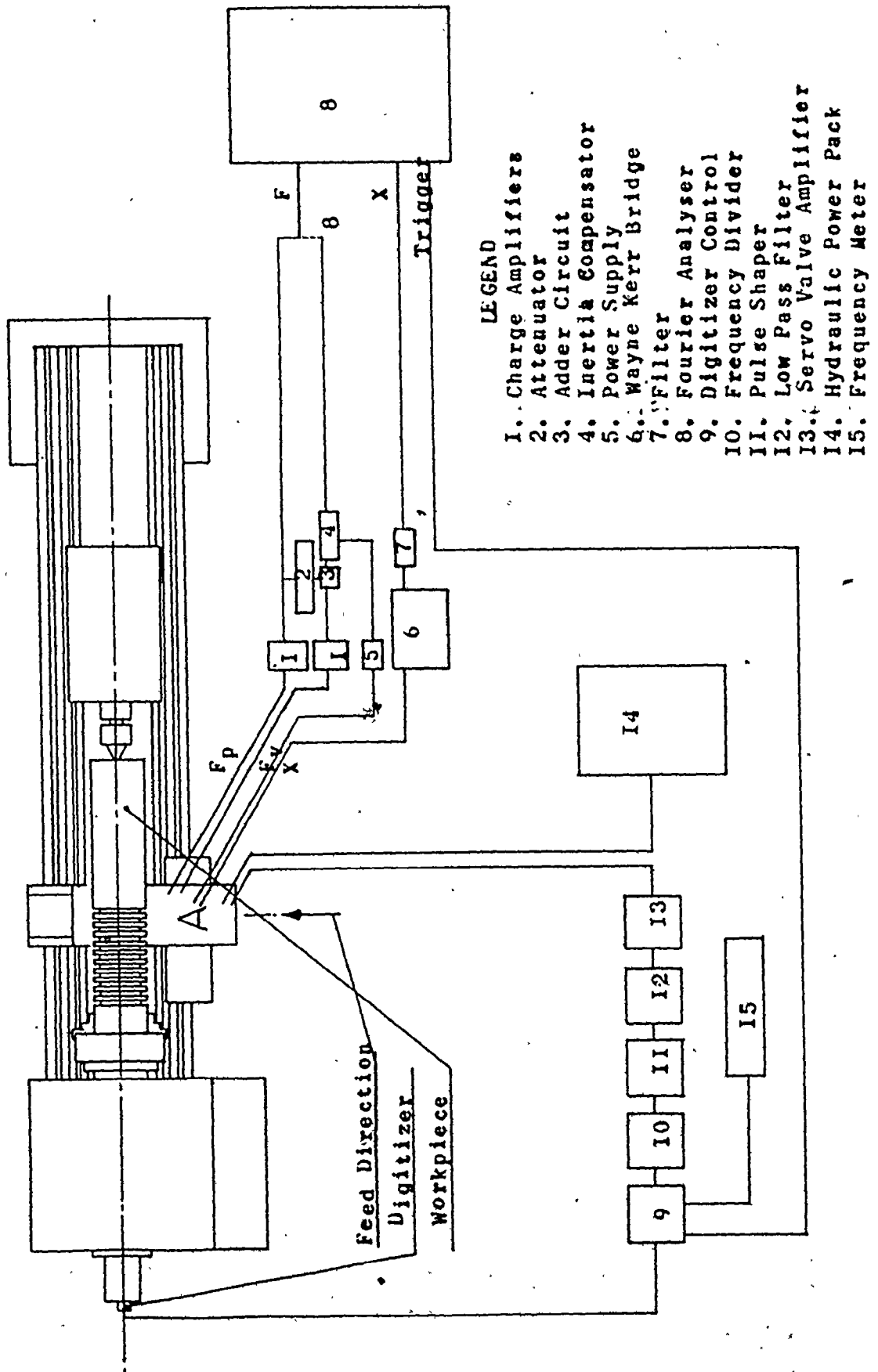


Fig. 3 MEASUREMENT SET-UP FOR THE DYNAMIC CUTTING FORCE COEFFICIENT

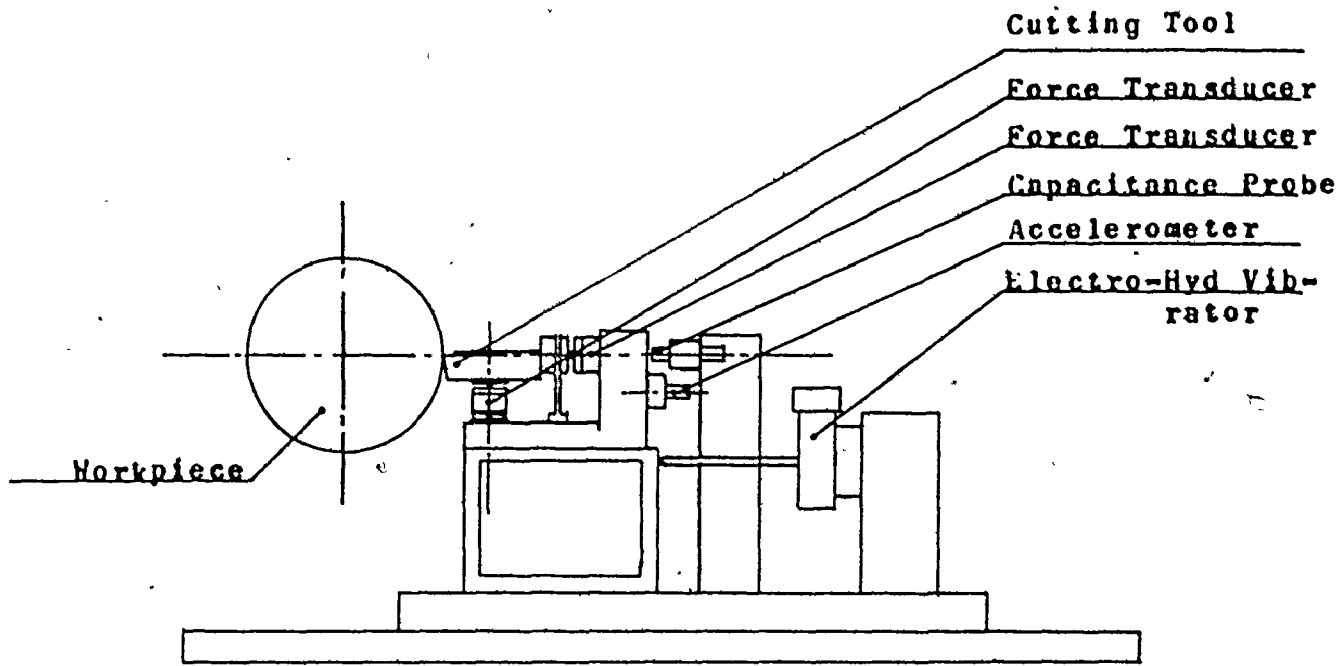


Fig.4 DETAIL 'A' (OF Fig.3)

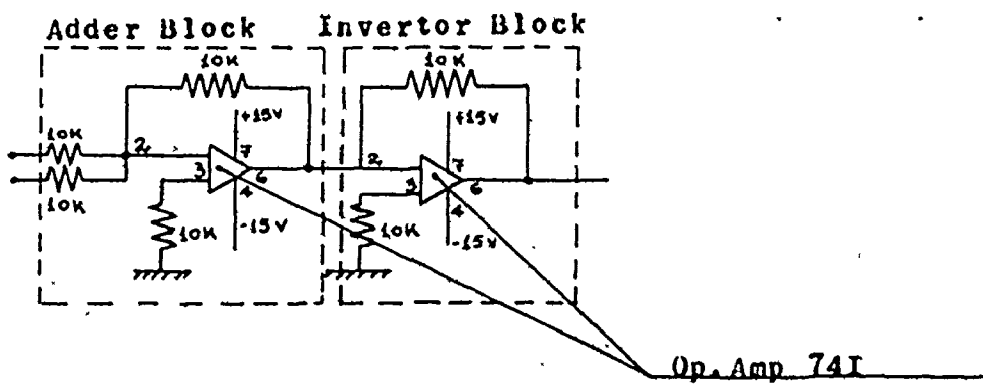
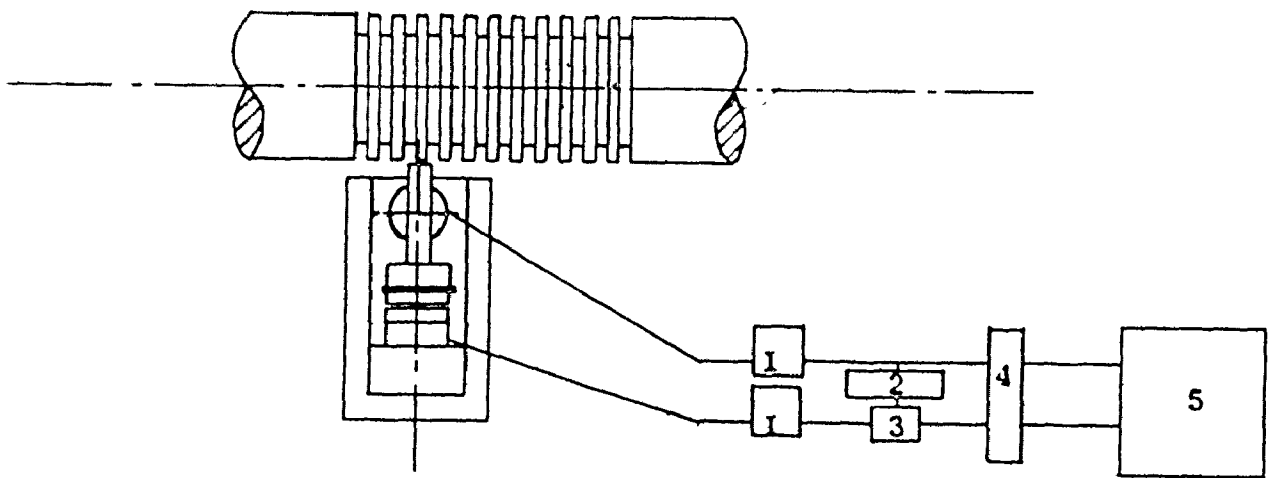


Fig.5 ADDER CIRCUIT



- LEGEND**
- 1. Charge Amplifiers
 - 2. Attenuator
 - 3. Adder Circuit
 - 4. Attenuator
 - 5. Pen Type Recorder

Fig.6 STATIC FORCE MEASUREMENT SET-UP

THRUST FORCE

Material 1020
 rake angle = 3°
 $V_B = 0.002''$
 $s = 0.0051''/\text{rev}$
 $f = 200\text{Hz}$

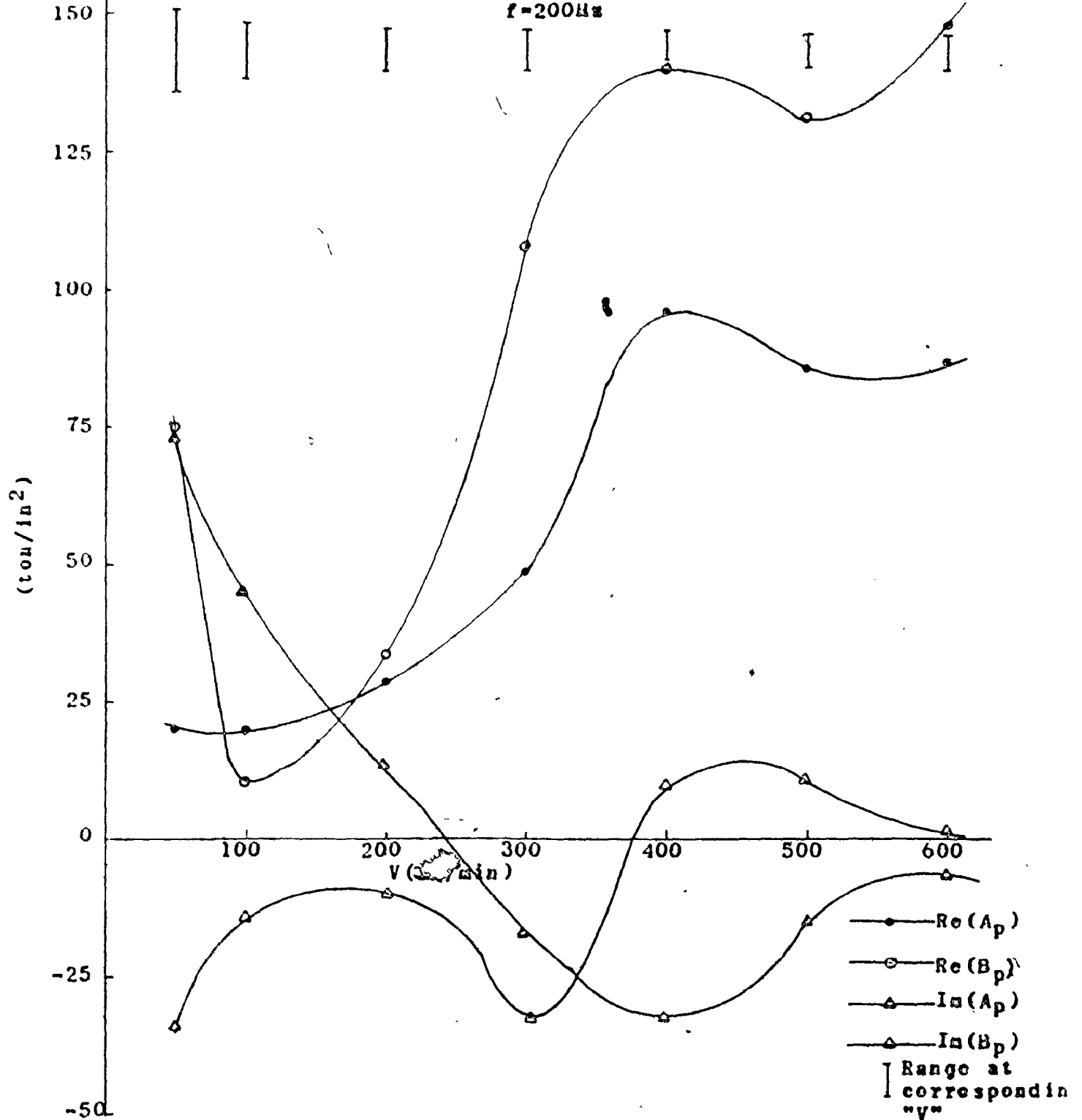


Fig. 7 VARIATION OF D.C.F.C.s WITH SPEED

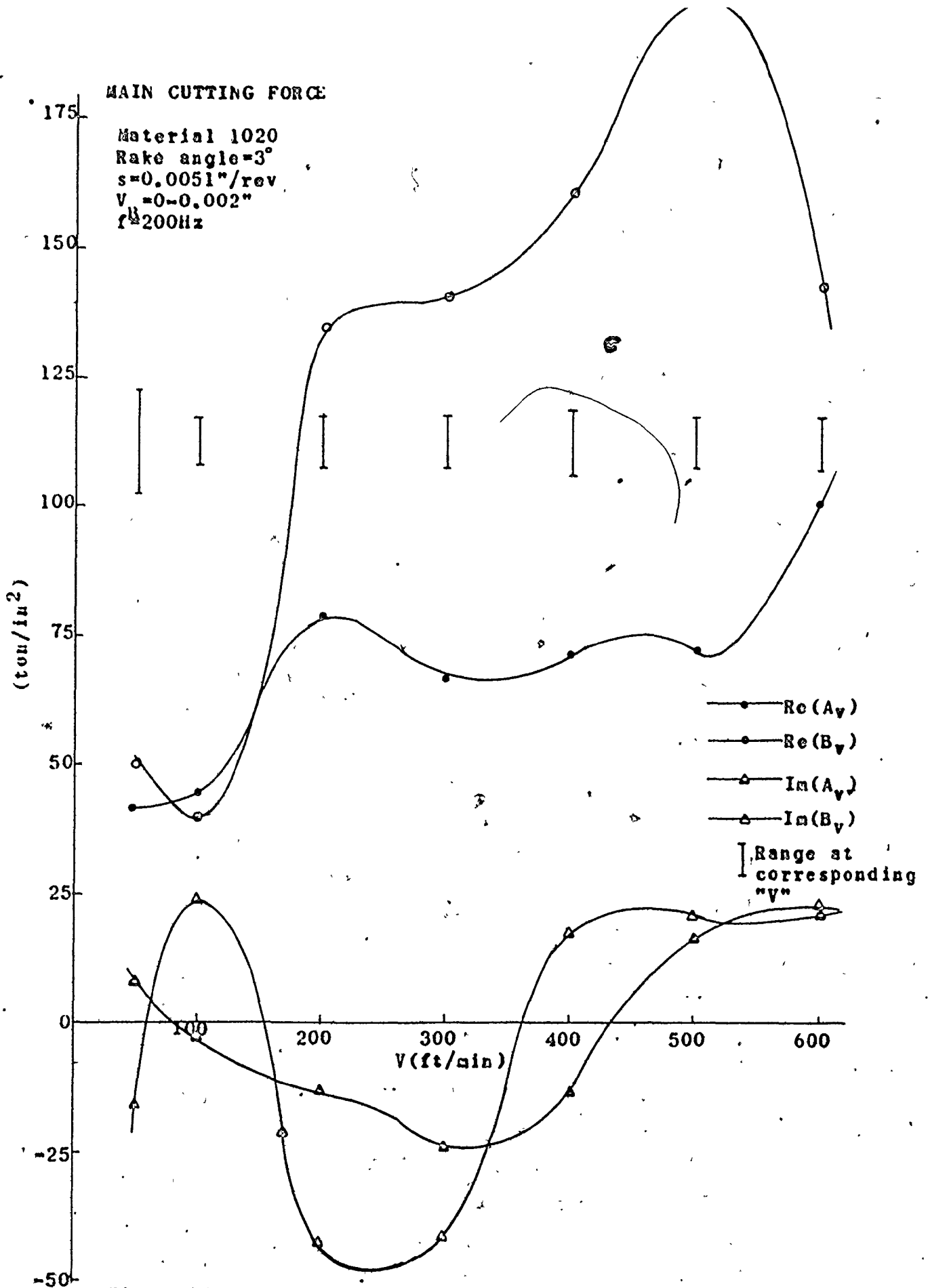


Fig. 8 VARIATION OF D.C.F.Cz WITH SPEED

THRUST FORCE

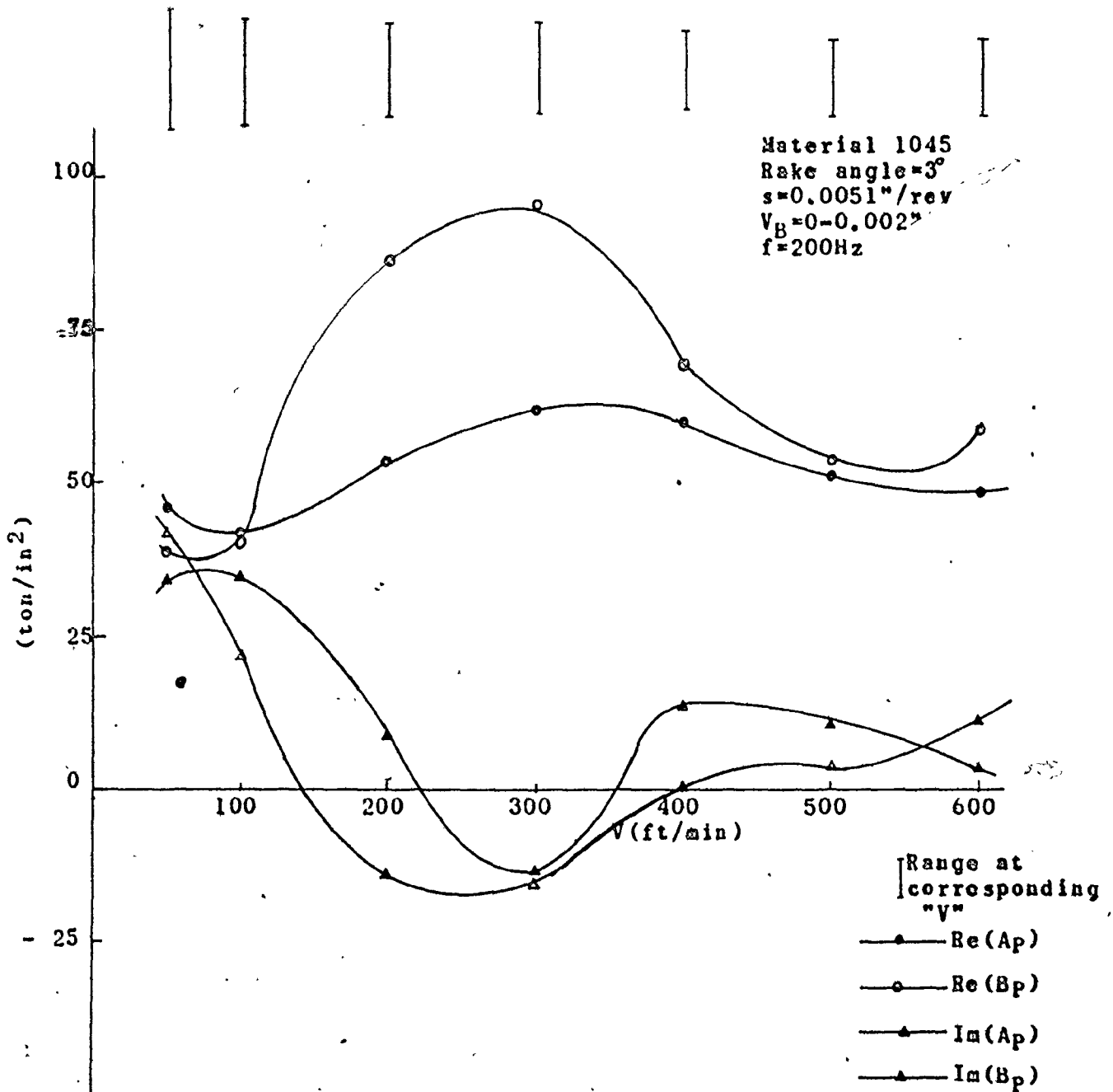


Fig. 9 VARIATION OF D.C.F.Cs WITH SPEED

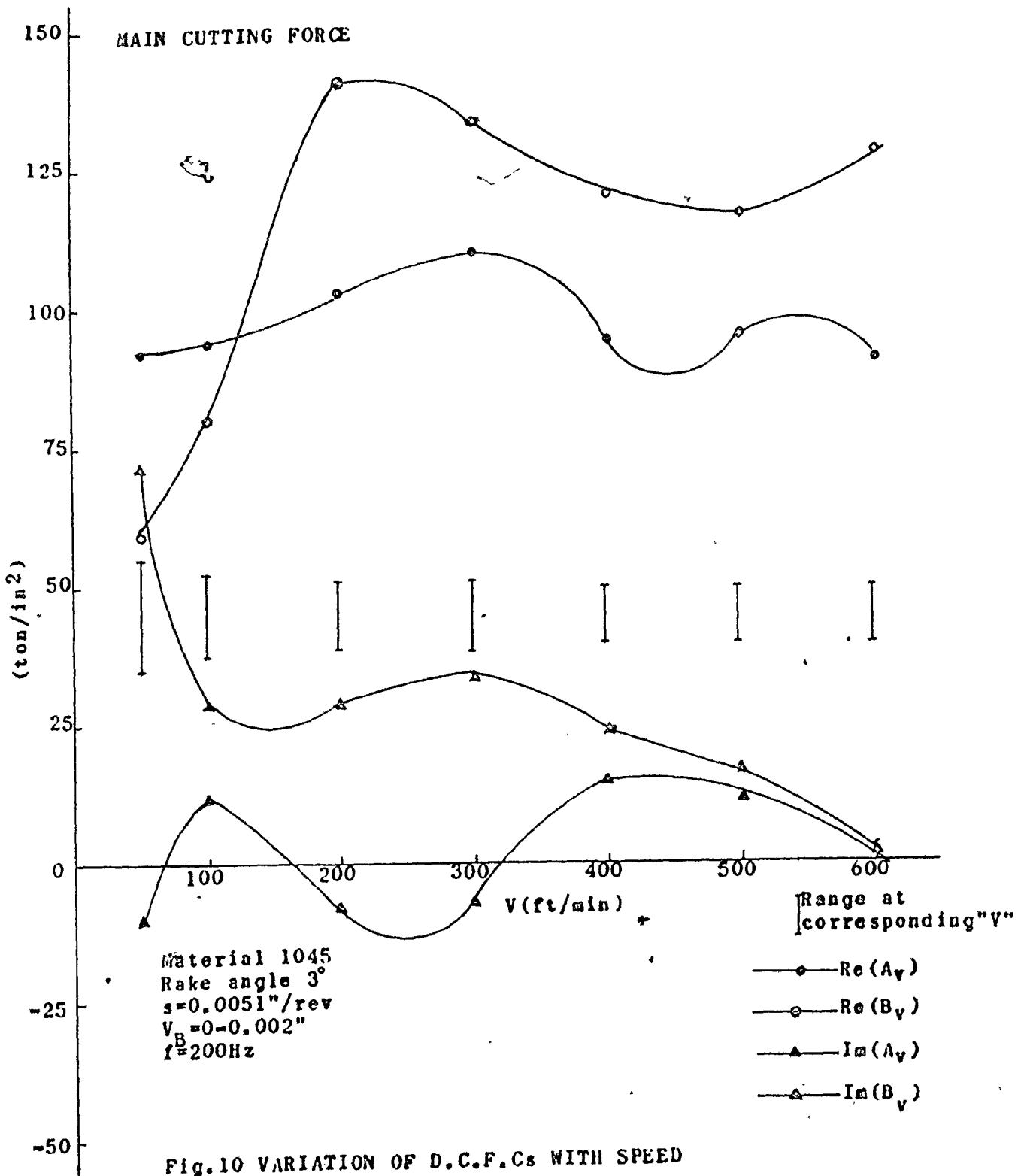


Fig. 10 VARIATION OF D.C.F.Cs WITH SPEED

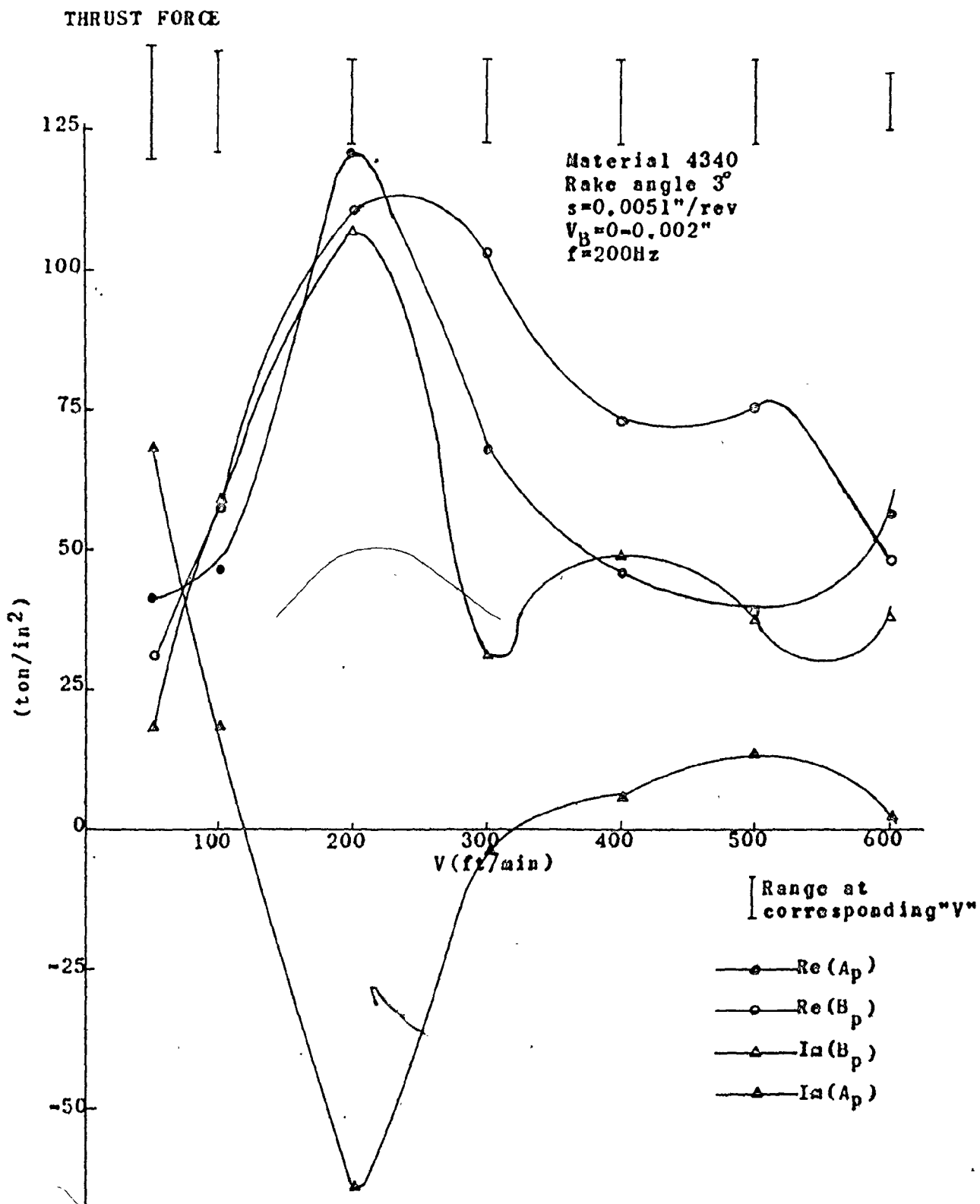


Fig. 11 VARIATION OF D.C.F.Cs WITH SPEED

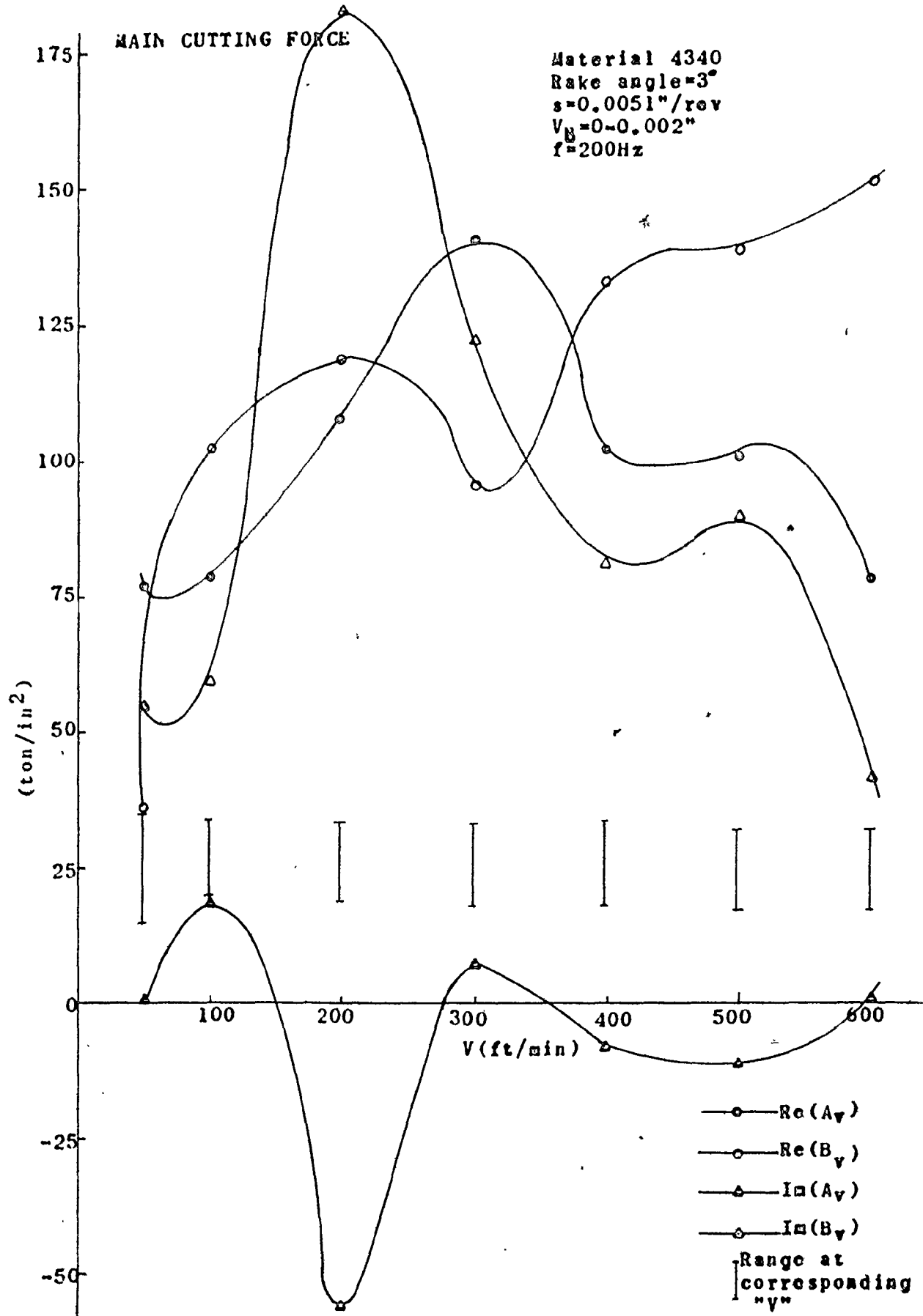


Fig.12 VARIATION OF D.C.F.s WITH SPEED

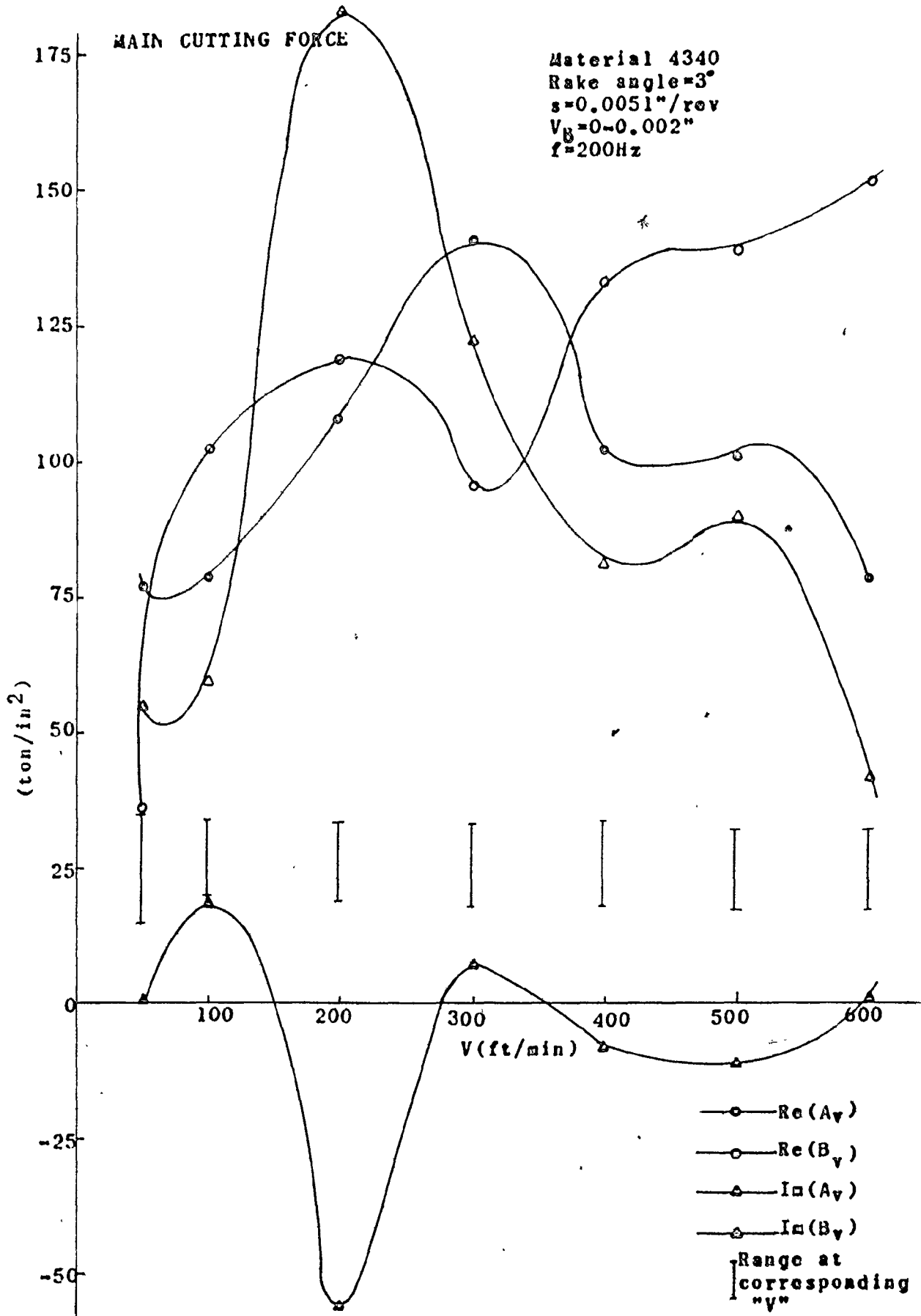


Fig.12 VARIATION OF D.C.F.Cs WITH SPEED

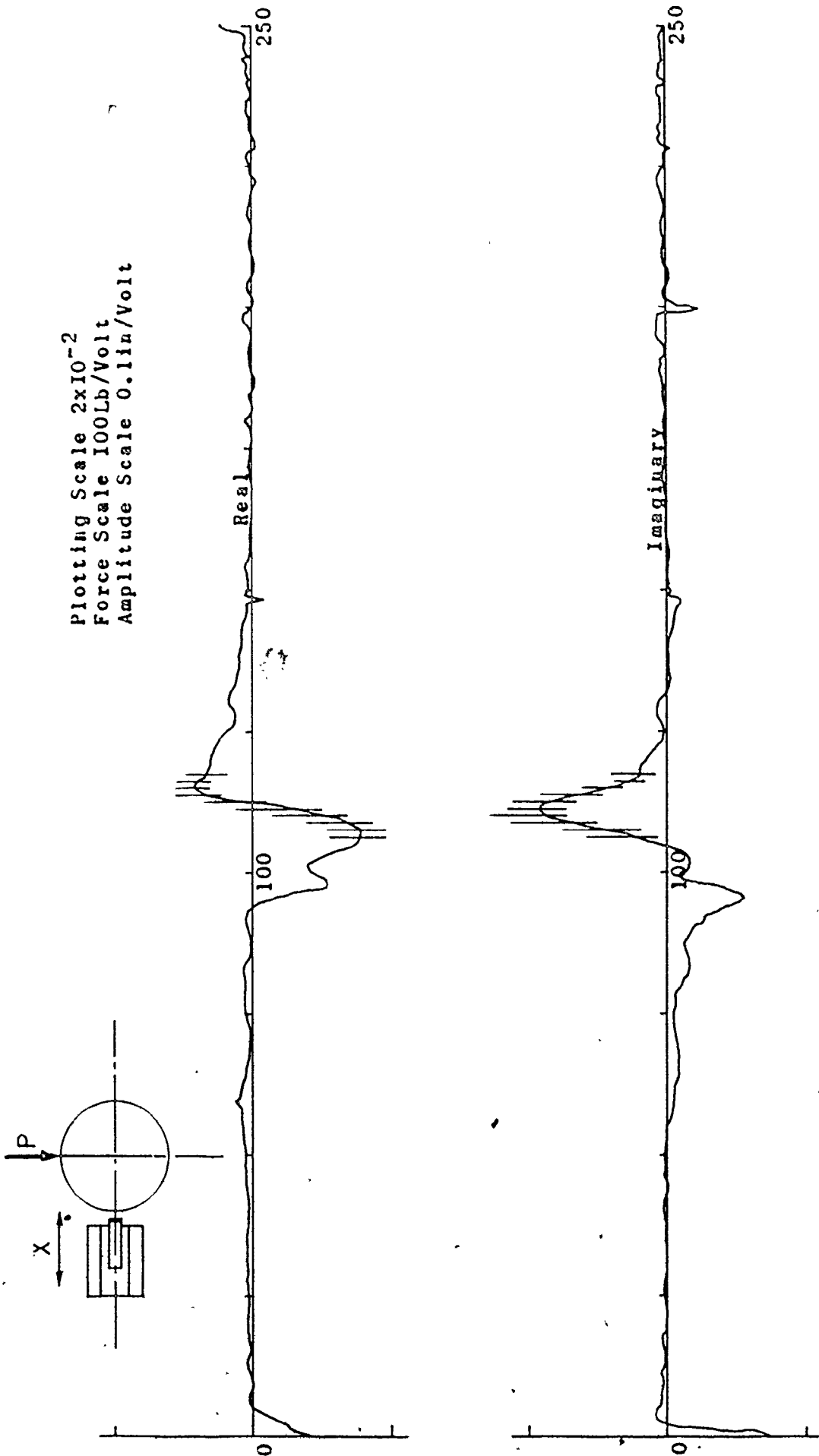
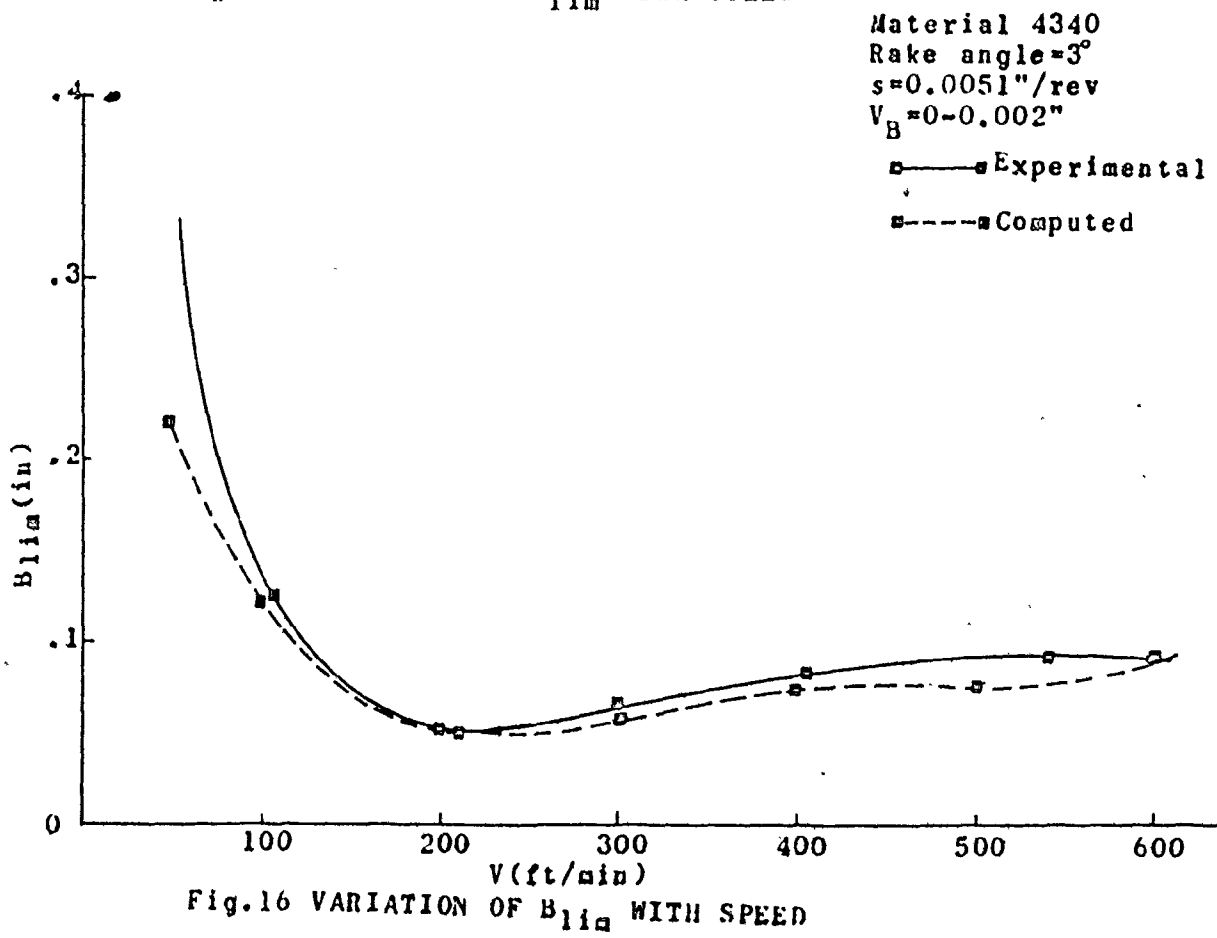
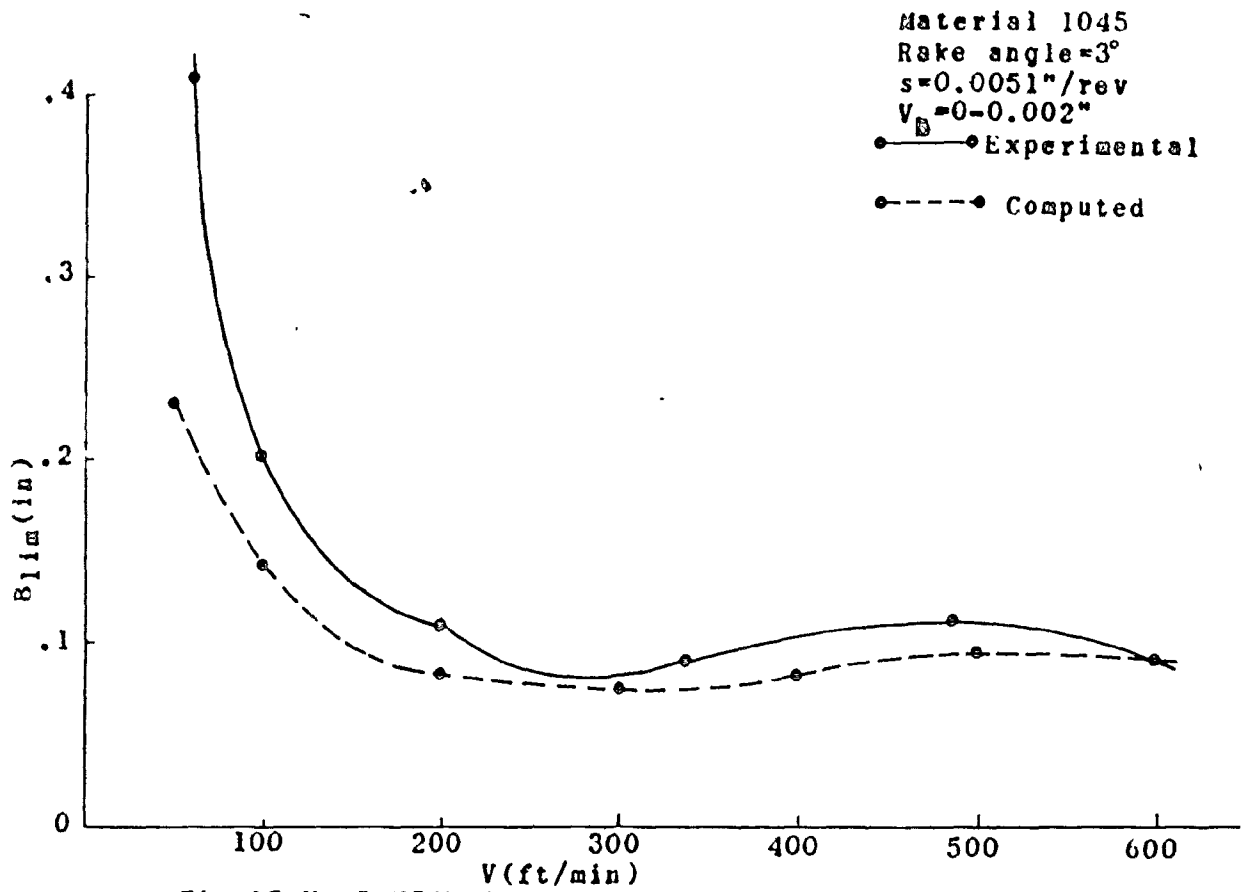


FIG. 14 HORIZONTAL CROSS RECEPTANCE OF TOS SN40-B LATHIL



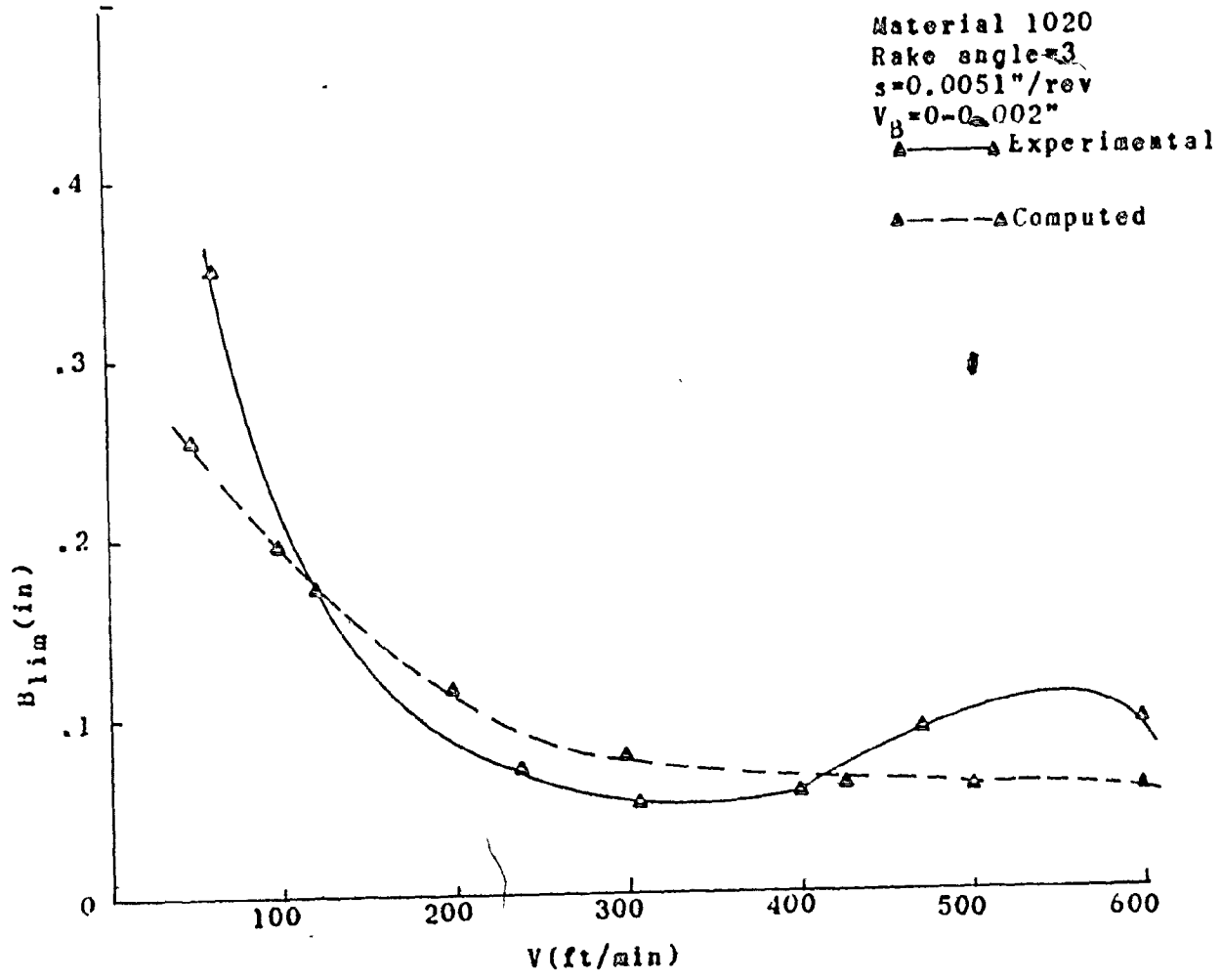


Fig.17 VARIATION OF B_{lim} WITH SPEED

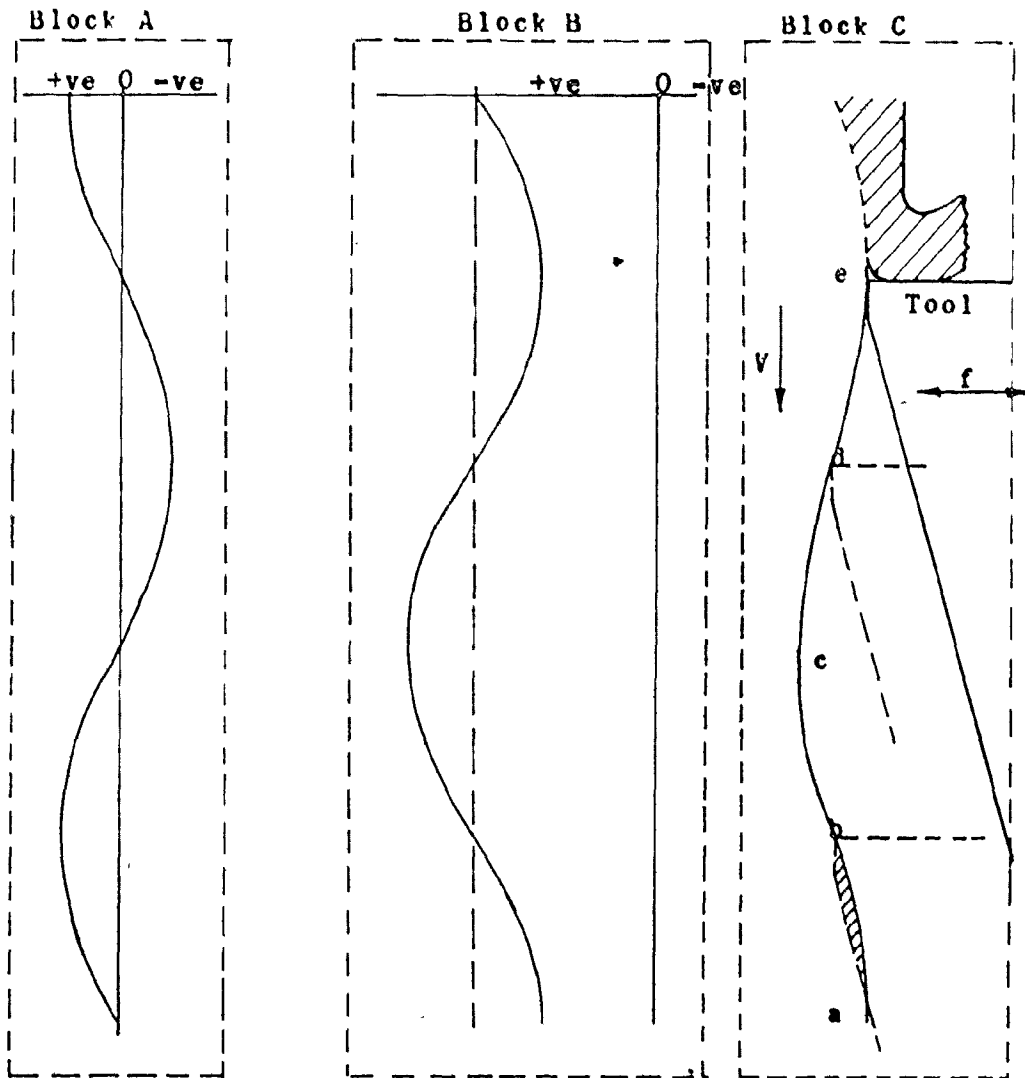


Fig.18 THE DYNAMIC PROCESS OF WAVE CUTTING

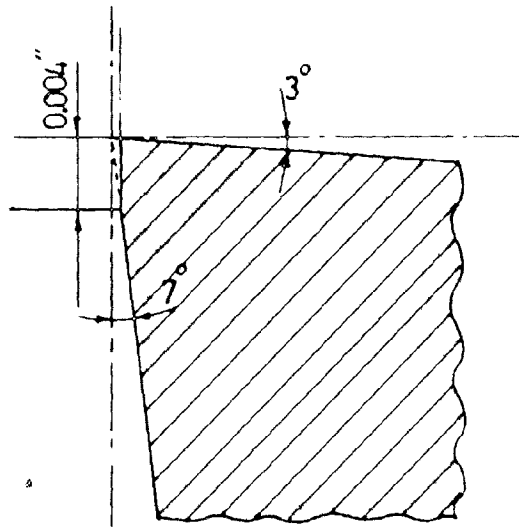


Fig.19 TOOL TIP WITH 0 DEGREE CLEARANCE

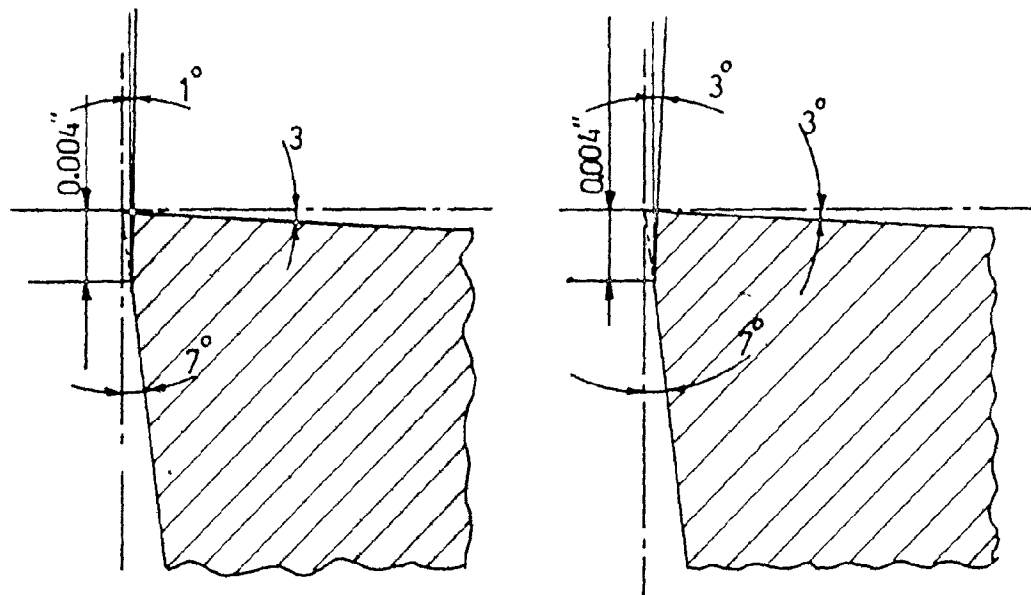


Fig.20 TOOL TIPS WITH NEGATIVE CLEARANCE

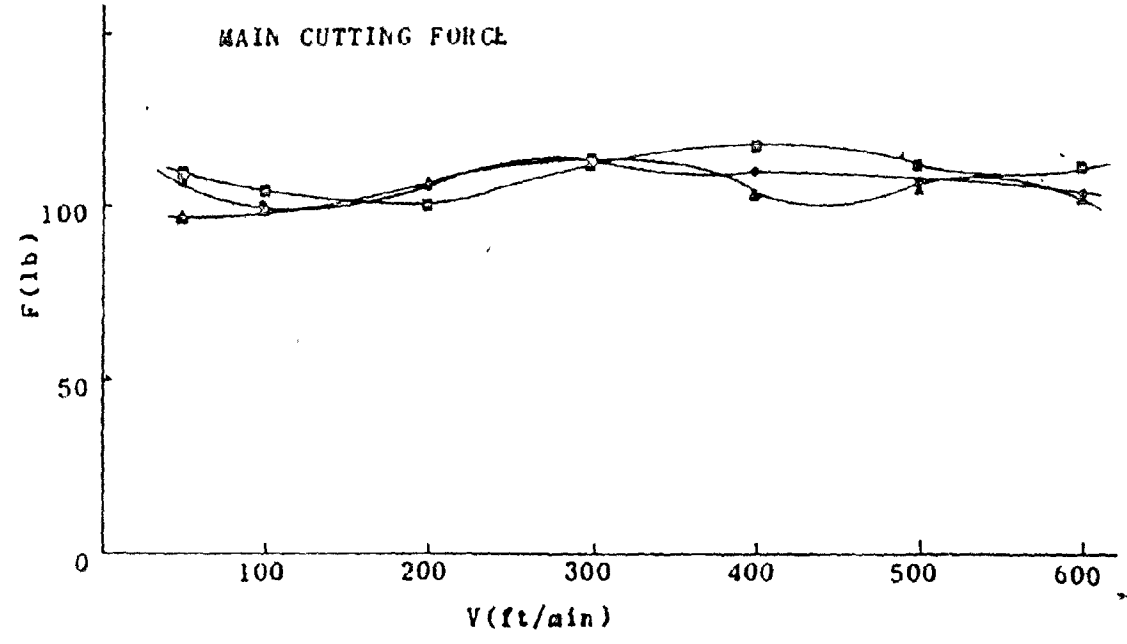
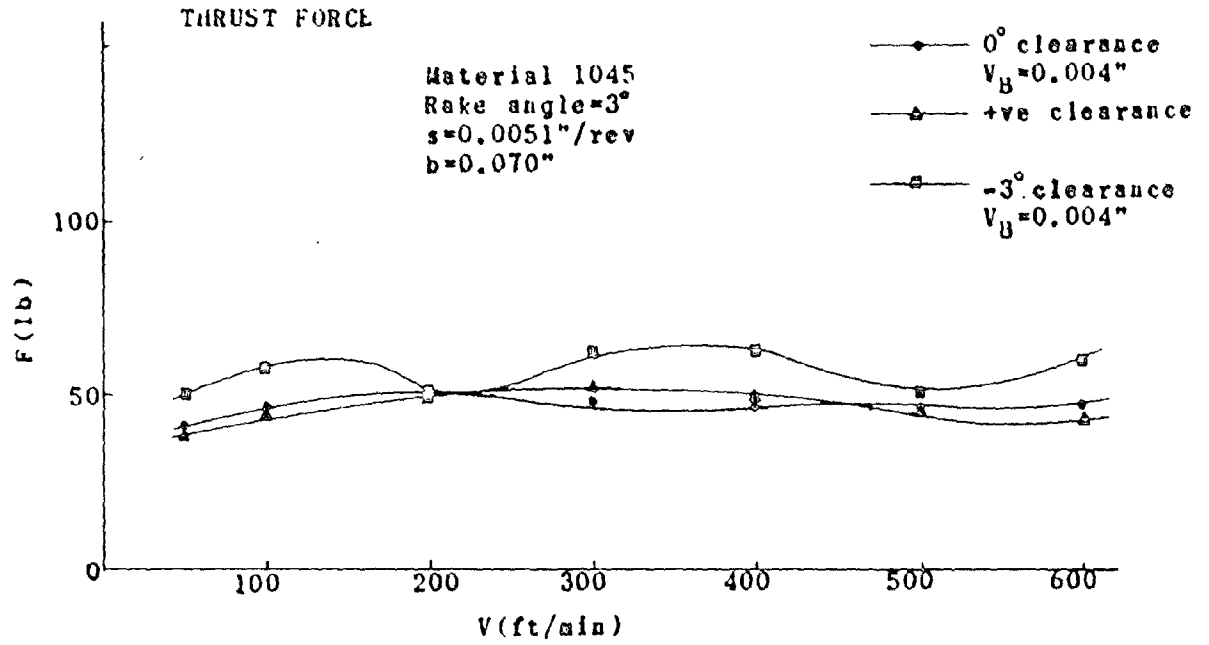


Fig.21 VARIATION OF STABLE CUTTING FORCES WITH SPEED

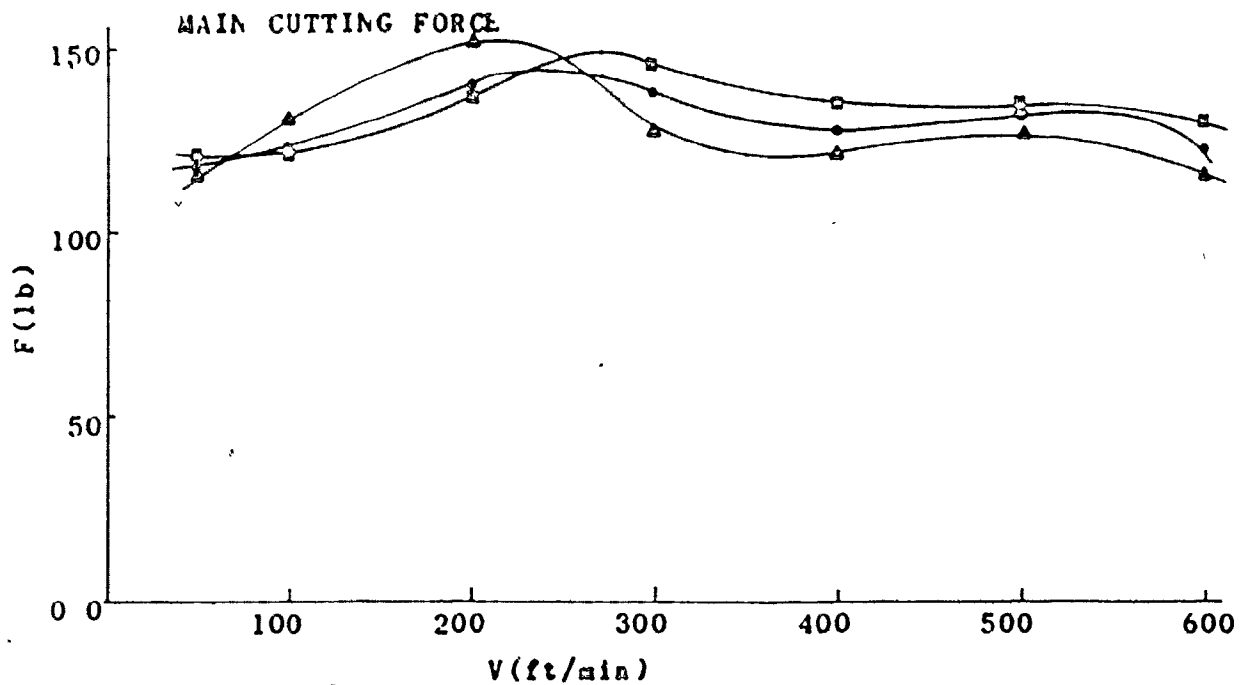
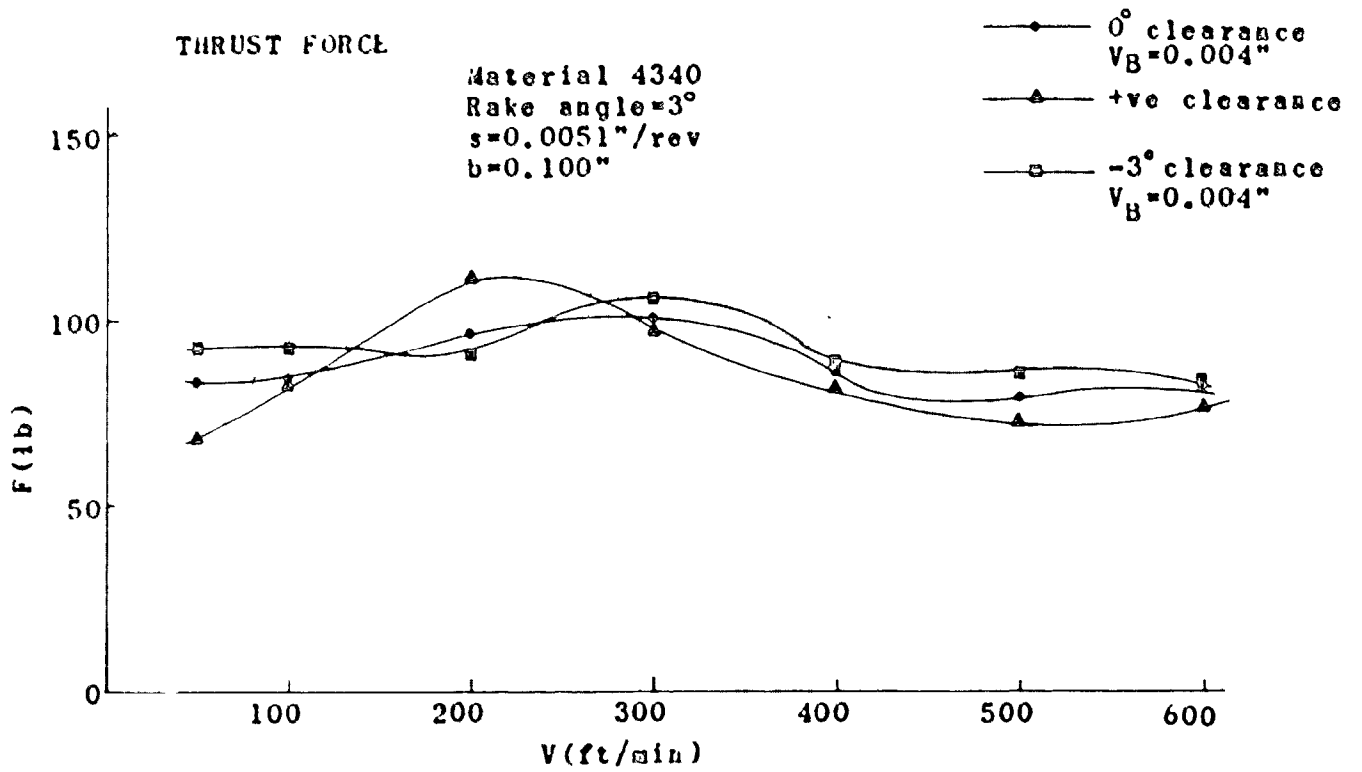


Fig.22 VARIATION OF STABLE CUTTING FORCES WITH SPEED

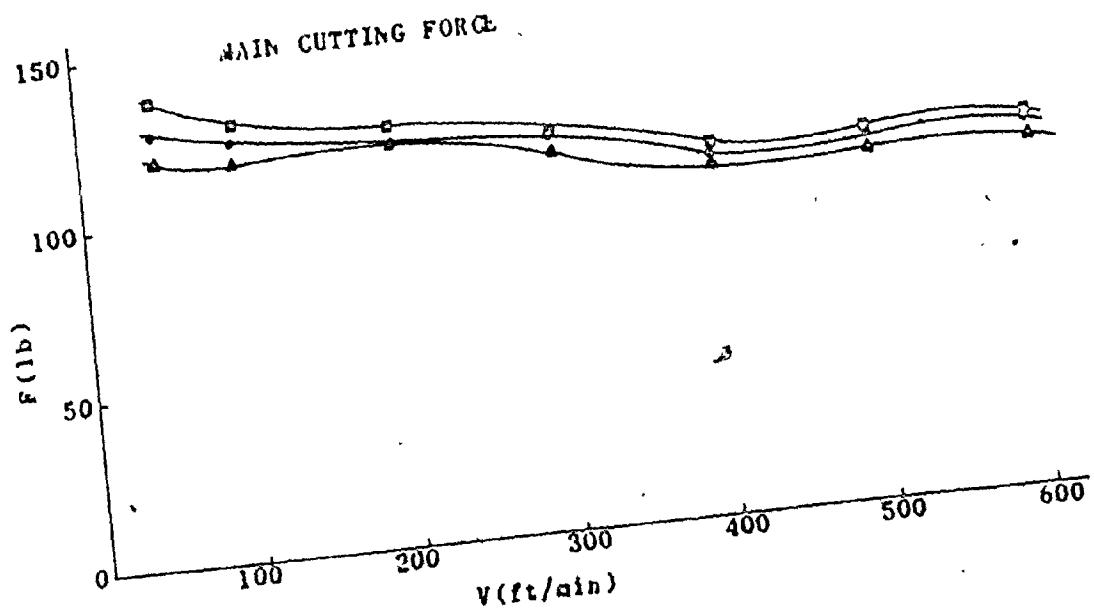
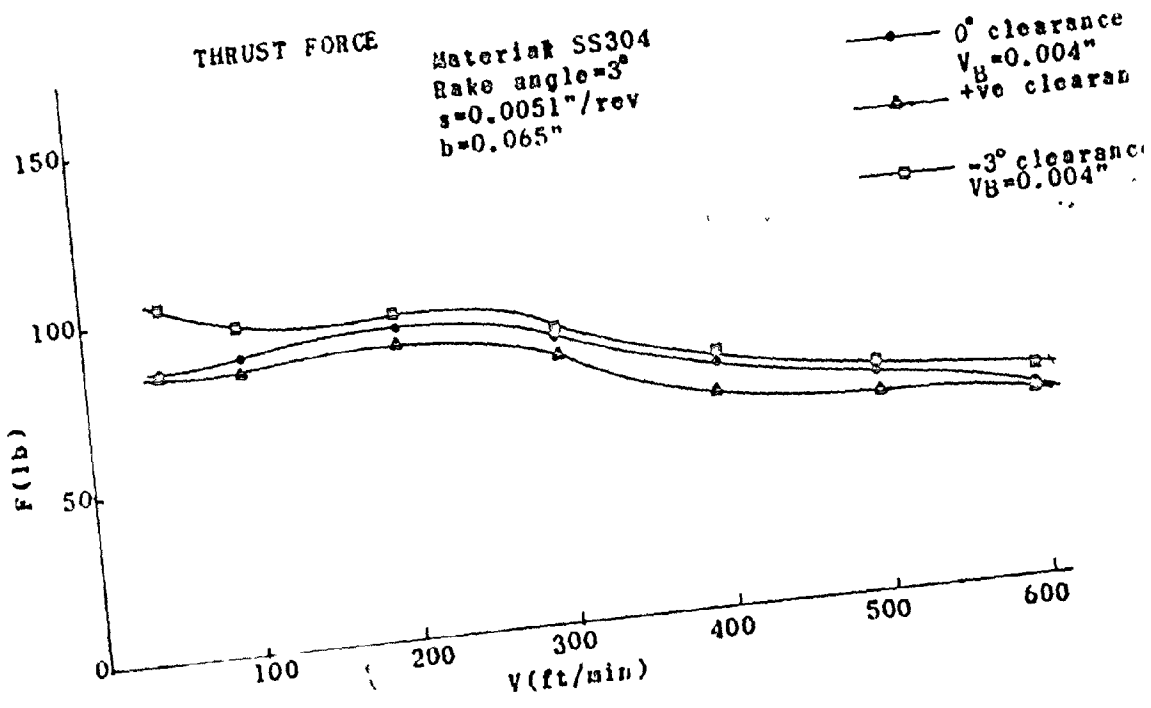


Fig. 23 VARIATION OF STABLE CUTTING FORCES WITH SPEED

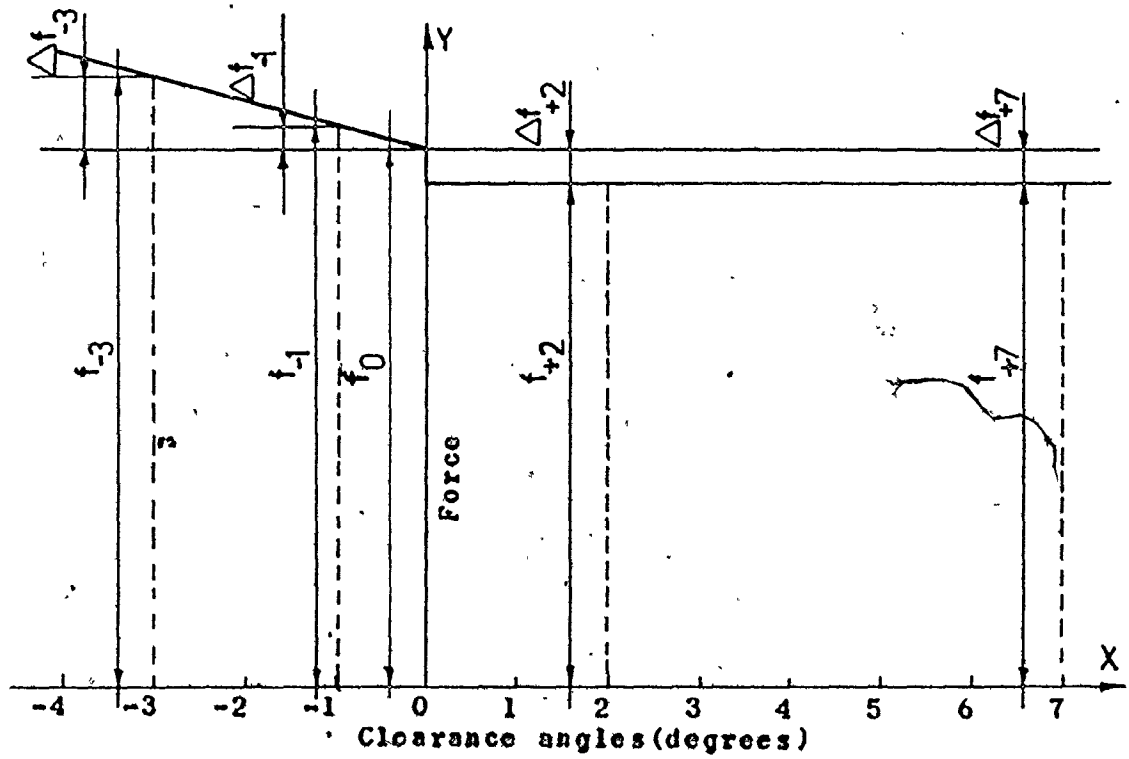


Fig.24 FORCE AND CLEARANCE ANGLE DIAGRAM FOR INNER MODULATION

THRUST FORCE

Material 1045
 Rake angle = 3°
 s = 0.0051"/rev
 f = 200Hz

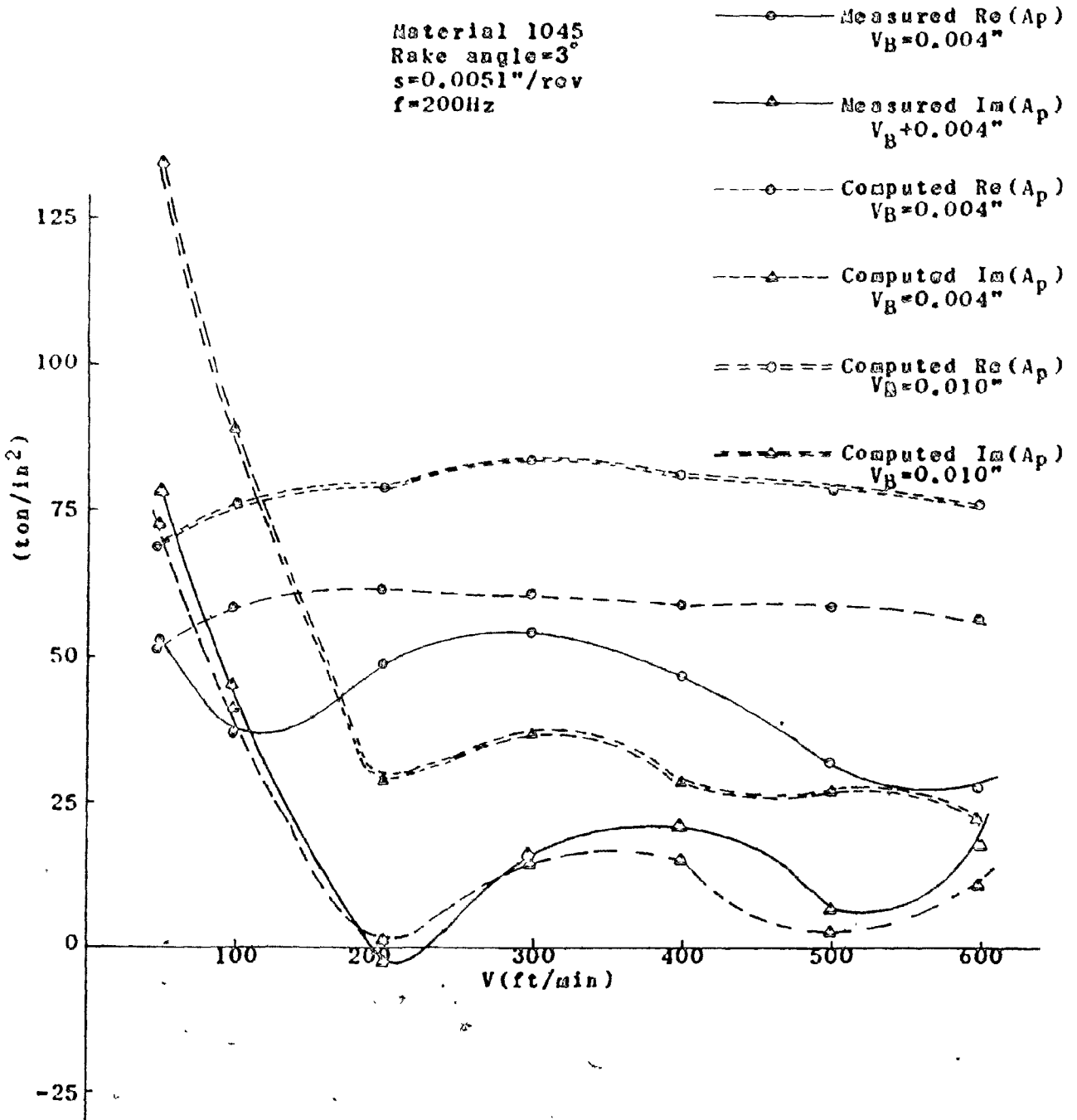


Fig. 25 VARIATION OF COMPUTED AND MEASURED D.C.F. C_m WITH SPEED

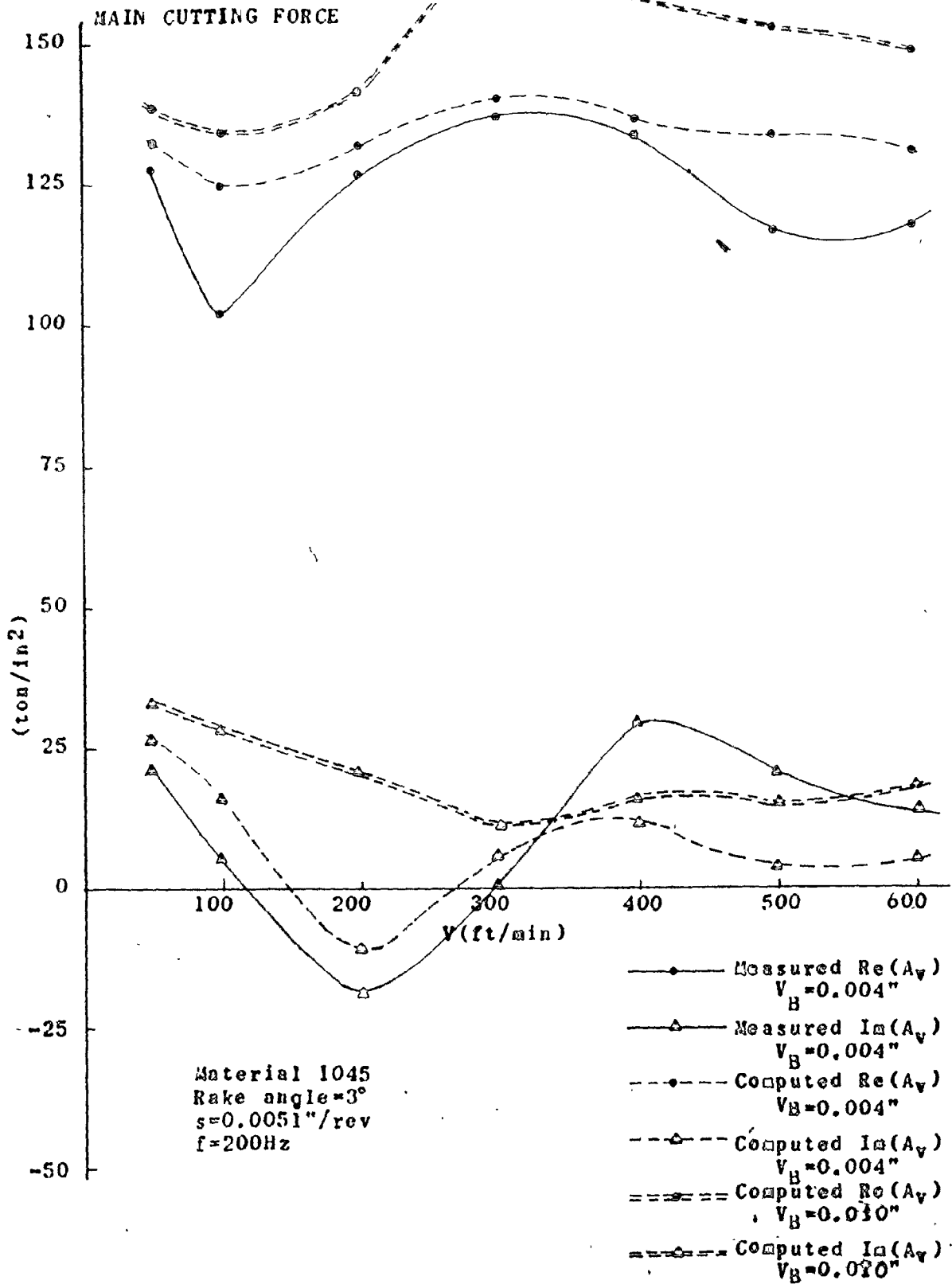


Fig. 26 VARIATION OF COMPUTED AND MEASURED D.C.F.s WITH SPEED

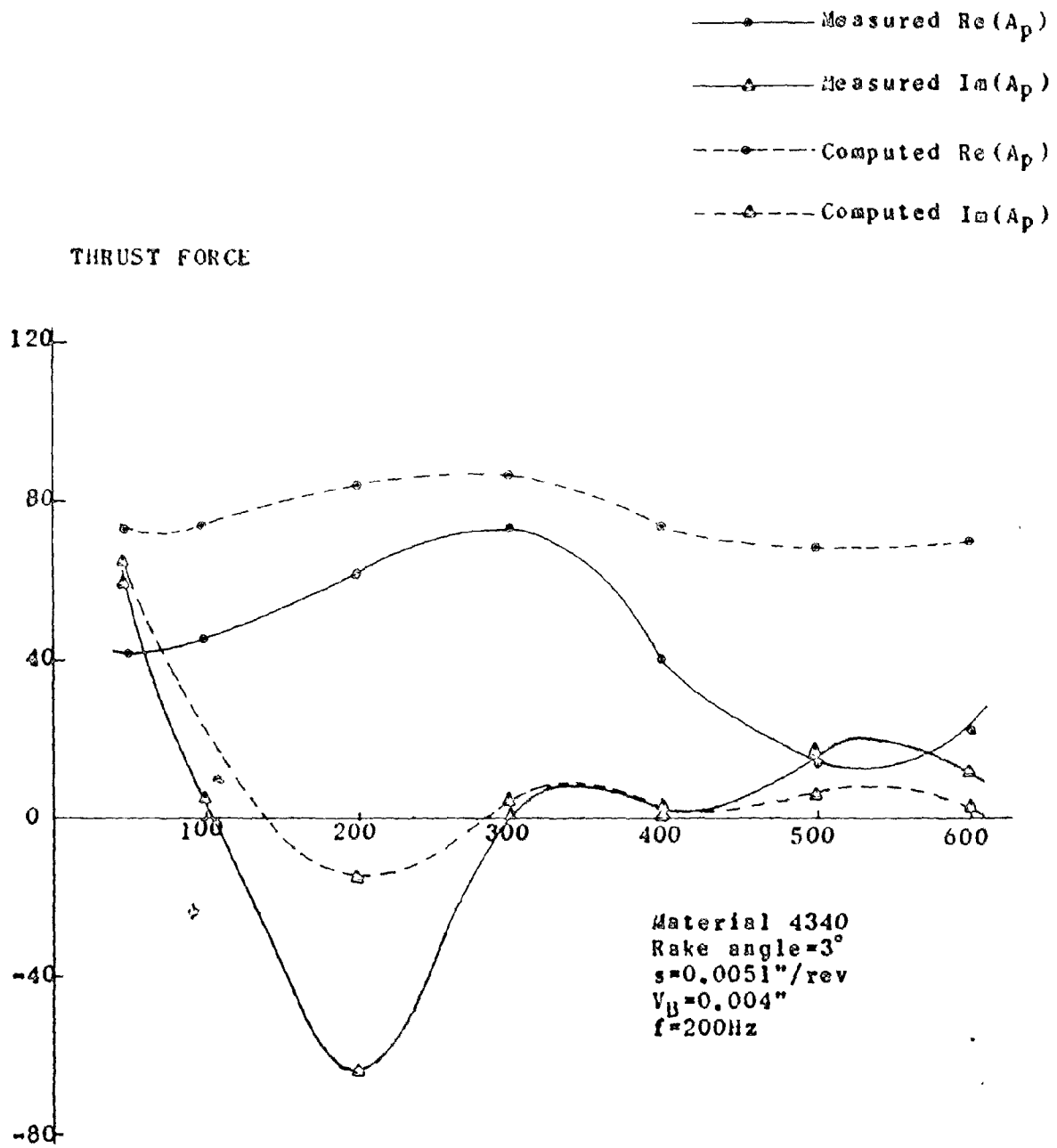


Fig.27 VARIATION OF COMPUTED AND MEASURED D.C.F.Cs WITH SPEED

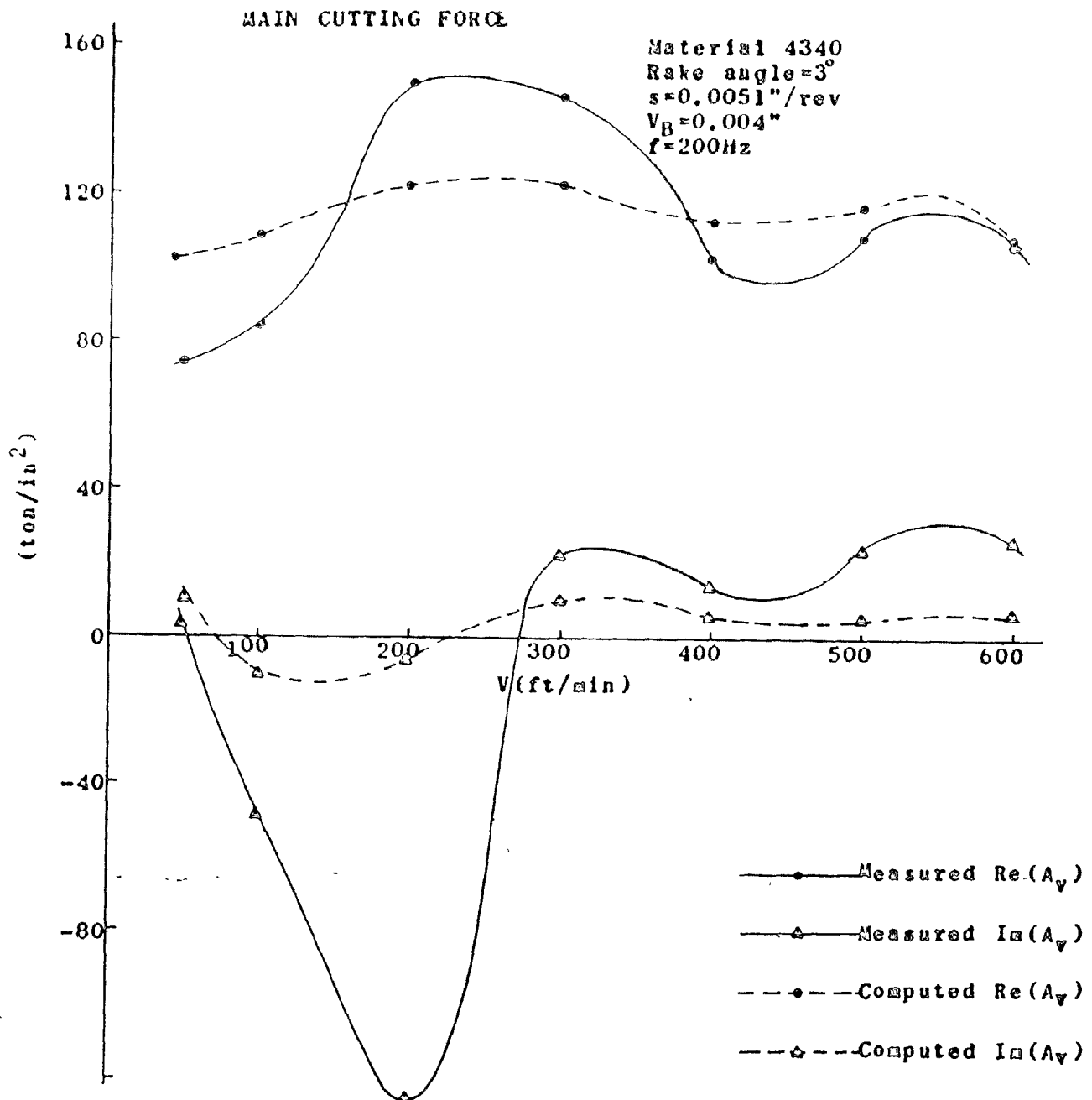


Fig. 28 VARIATION OF COMPUTED AND MEASURED D.C.F.Cs WITH SPEED

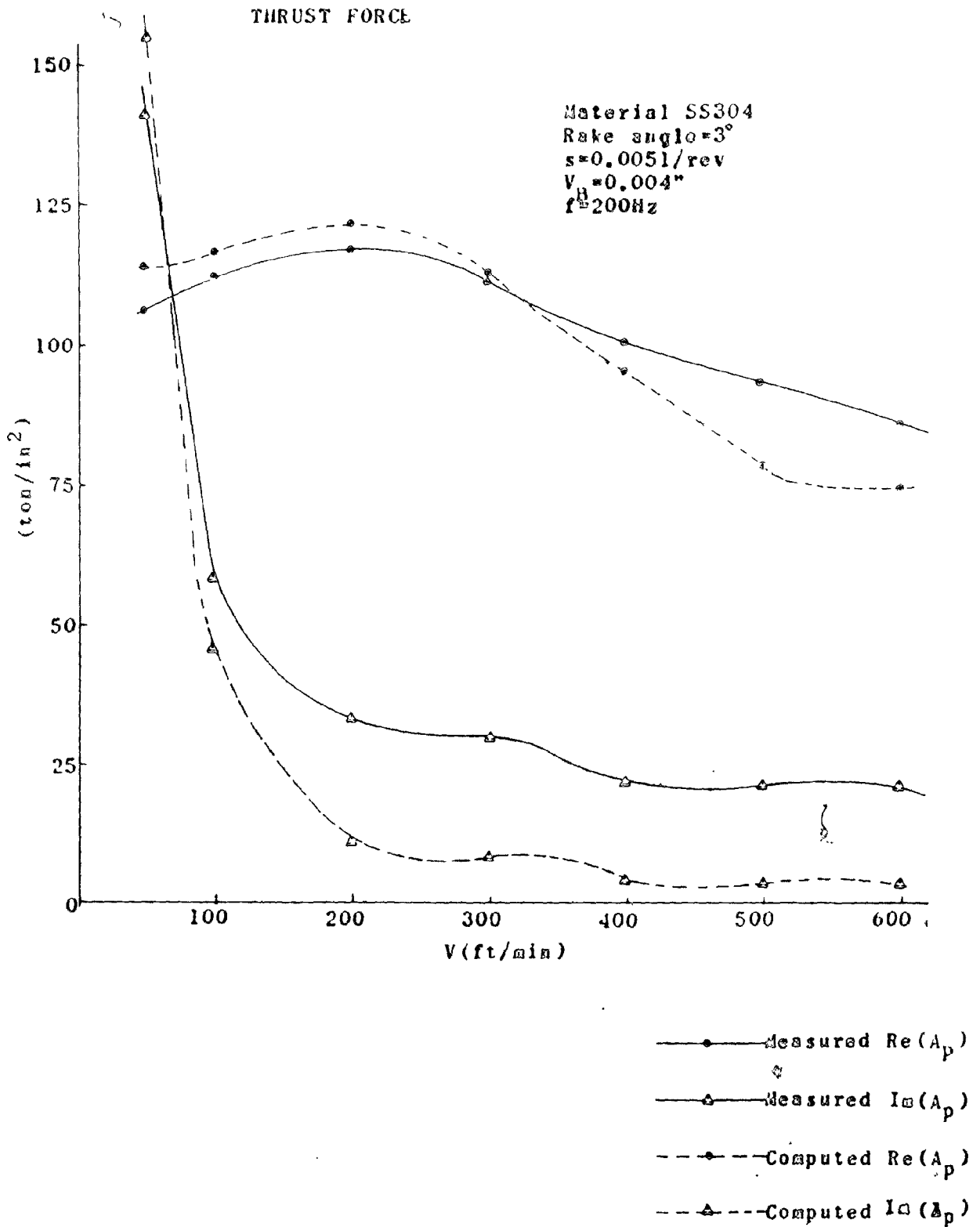


Fig. 29 VARIATION OF COMPUTED AND MEASURED D.C.F.C.s WITH SPEED

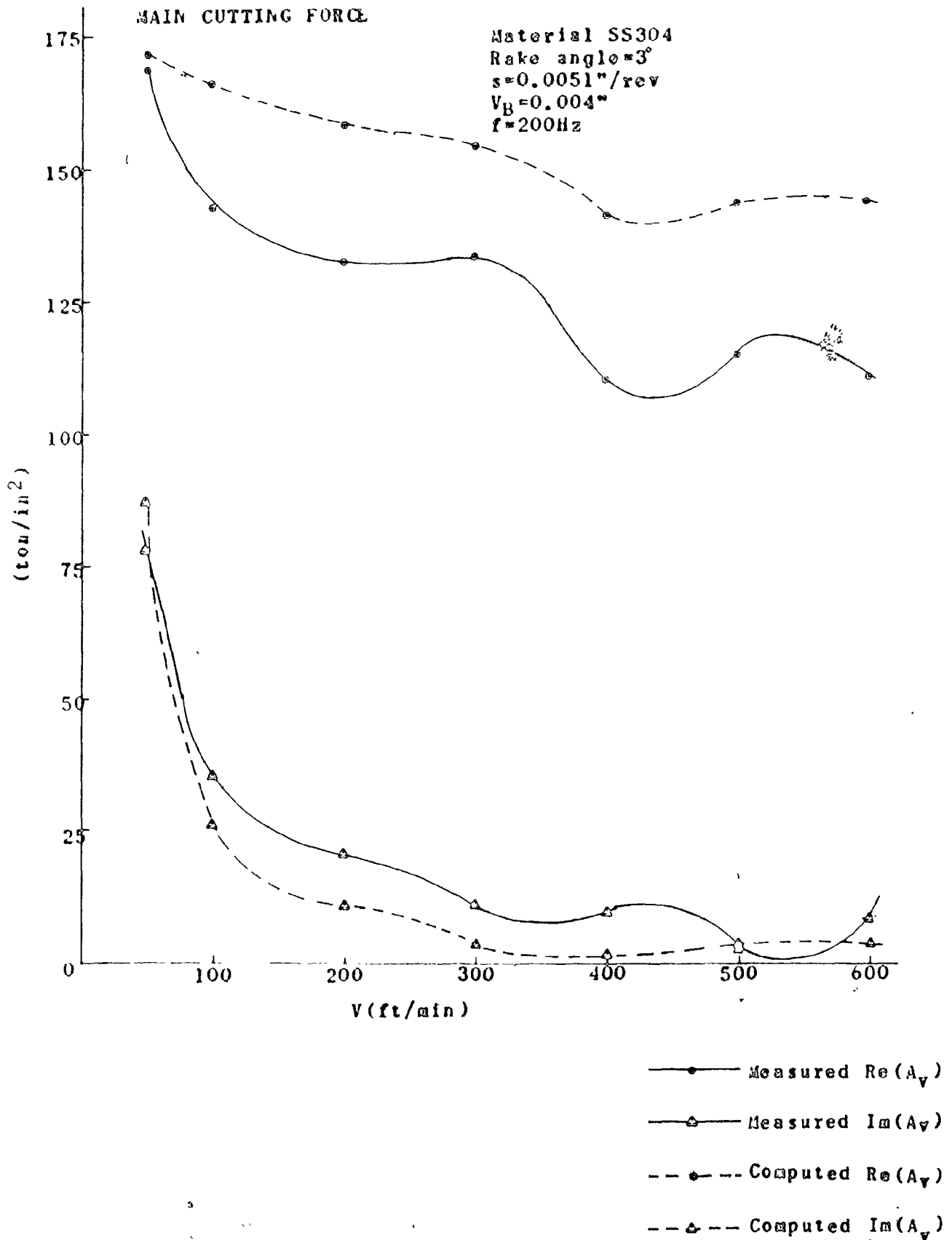


Fig. 30 VARIATION OF COMPUTED AND MEASURED D.C.F.C.s WITH SPEED